Homogenization of Surface Energy and Elasticity for Highly Rough Surfaces

Dajla Neffati
Department of Mechanical Engineering,
University of Houston,
Houston, TX 77204
e-mail: dajla.neffati@gmail.com

Yashashree Kulkarni[1]
Department of Mechanical Engineering,
University of Houston,
Houston, TX 77204
e-mail: ykulkarni@uh.edu

Surface energy plays a central role in several phenomena pertaining to nearly all aspects of materials science. This includes phenomena such as self-assembly, catalysis, fracture, void growth, and microstructural evolution among others. In particular, due to the large surface-to-volume ratio, the impact of surface energy on the physical response of nanostructures is nothing short of dramatic. How does the roughness of a surface renormalize the surface energy and associated quantities such as surface stress and surface elasticity? In this work, we attempt to address this question by using a multi-scale asymptotic homogenization approach. In particular, the novelty of our work is that we consider highly rough surfaces, reminiscent of experimental observations, as opposed to gentle roughness that is often treated by using a perturbation approach. We find that softening of a rough surface is significantly underestimated by conventional approaches. In addition, our approach naturally permits the consideration of bending resistance of a surface, consistent with the Steigmann–Ogden theory, in sharp contrast to the surfaces in the Gurtin–Murdoch surface elasticity theory that do not offer flexural resistance. [DOI: 10.1115/1.4053081]

Keywords: homogenization, multi-scale asymptotics, surface roughness, surface elasticity, constitutive modeling of materials, elasticity

1 Introduction

From an atomistic perspective, a surface is essentially a defect as it disrupts the atomic order in the material. Atoms on a free surface have different arrangement of neighbors, or coordination number, than their counterparts in the bulk. Therefore, if we regard a surface as layer(s) of atoms that differ from atoms in the interior, it is reasonable to expect that the physical properties associated with surfaces would be distinct from those of the bulk of the same material. By virtue of these atomistic underpinnings, surfaces play a vital role in several phenomena pertaining to nearly all aspects of material behavior. Furthermore, as the surface-to-volume ratio becomes significantly large at small scales, the impact of surfaces on the physical response of nanostructures is nothing short of dramatic. With the advent of nanotechnology and the drive toward miniaturization, surface energy-related effects have gained prominence in recent decades and have been studied in a wide range of contexts such as catalysis [1–3], sensing and vibrations [4–6], composites [7–10], self-assembly [11], phase transformation [12,13], fracture [14], nanostructures [15–23], and even fluid mechanics [24], soft materials [25–27], and biology [28,29].

In continuum mechanics, surface effects are usually modeled following the theoretical framework for surface elasticity pioneered by Gurtin and Murdoch [30,31,28,9]. The surfaces are regarded as elastic membrane-like entities with zero thickness attached to the bulk and endowed with a non-trivial excess energy referred to as the surface energy (see Ref. [32]). In the case of solids, the surface energy consists of two primary contributions. The first contribution is akin to capillarity or surface tension in fluids but is known as surface stress in the context of solids. The second contribution comes from surface elasticity as we need to account for the energetic cost associated with the elastic response of a solid surface. Since this area has been very well-studied, we refer to a few recent articles that provide an excellent literature review [2,23,32–36]. Some studies have also investigated the role of surface energy in the context of imperfect interfaces by treating them as a thin elastic membrane [37,38].

The importance of curvature-dependence of surface energy was first propounded by Steigmann and Ogden [39,40]. They demonstrated that the theoretical framework of Gurtin–Murdoch is incapable of modeling equilibrium deformations involving compressive surface stress fields as it does not account for elastic resistance to flexure. Naturally then, they argued, the Gurtin–Murdoch theory cannot be used to simulate local surface features, such as in wrinkling or roughening, which result from compressive surface stresses. Steigmann and Ogden proposed a modified framework which resolved this issue by incorporating curvature-dependent surface energy. However, due to the complexity of the Steigmann–Ogden curvature-dependent surface elasticity, there are very few studies on this topic till date [41–43]. Fried and Todres [41] analyzed wrinkling instability of a soft film subjected to the action of van der Waals force whereas Schiavone and Ru [42] examined the solvability of Steigmann–Ogden theory applied to plane-strain boundary value problems. Chhapadia et al. [43] applied the Steigmann–Ogden theory as well as atomistic simulations to provide a resolution to the apparent anomalous bending behavior of nanostructures.

The continuum theory of surfaces assumes a smooth, flat surface attached to the bulk. However, the surfaces of most real materials, even highly polished ones, exhibit roughness across various length scales. This raises an intriguing question: what is the impact of roughness on surface energy and its role in mechanical and other properties? This question was investigated in a few studies [44,45,23,46]. In particular, Mohammadi et al. [46] approached this problem using an elegant homogenization scheme based on energetics. They considered gently rough surfaces (that is, surfaces with small amplitude waviness) and, hence, were able to use a perturbation method for their homogenization approach. They concluded that even gentle roughness dramatically alters surface elastic properties, although it has a negligible effect on residual surface stress. They also observed that even if the bare surface has

[1]Corresponding author.

Manuscript received October 16, 2021; final manuscript received November 17, 2021; published online December 21, 2021. Assoc. Editor: Yonggang Huang.

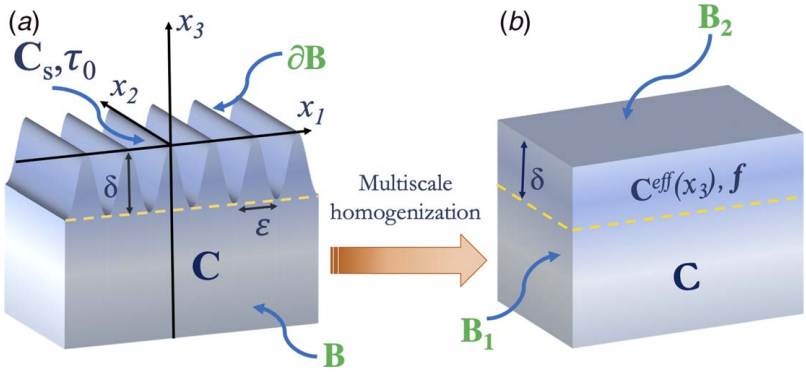

Fig. 1 Homogenization process of (*a*) a domain B with a stiffness tensor C and a rough surface ∂B with a stiffness tensor $\mathbf{C}_s$ and residual stress τ_0, an amplitude δ and period ϵ in the $x_1x_2x_3$ domain, (*b*) homogenized structure consisting of a domain B_1 with a stiffness tensor C topped by a layer B_2 of thickness δ characterized by an effective tensor $\mathbf{C}^{eff}$ varying along x_3 and subject to body forces

a zero surface elasticity modulus, roughness endows it with a finite modulus, and more importantly, some moduli may also change sign.

If gentle roughness can drastically renormalize the surface properties, what is the impact of highly rough surfaces? Addressing this question is the focus of our study. Using a multi-scale homogenization approach inspired by the work of Nevard and Keller [47], we seek to elucidate the effect of a very rough surface possessing surface elasticity. The central assumption underlying this method is that the wavelength of the roughness is small compared with the roughness amplitude which results in a highly rough surface. The significance of the multi-scale homogenization is that it replaces the highly rough surface with an equivalent layer of finite thickness with effective bulk properties that depend on the roughness as well as surface energy (see schematic in Fig. 1). This is in contrast to homogenization based on perturbation theory which yields an equivalent system consisting of a bulk and a flat (zero-thickness) surface with effective surface properties. In other words, the homogenized system furnished by multi-scale asympototics is a composite with distinct properties in the bulk and the effective layer. A unique advantage of the method is that it allows us to invoke the Steigmann–Ogden theory to examine the renormalized curvature-dependent surface elastic constants for a highly rough surface. Due to the small wavelength assumption, this method may not be suitable for modeling weak roughness where the wavelength is much larger than the roughness amplitude.

Some prior studies on homogenization of rough surfaces have been particularly crucial for the development of our work. Our proposed model differs from them in the following aspects:

(i) In the framework of Mohammadi et al. [46], the amplitude of the rough surface is small compared to the wavelength. Thus, the roughness is gentle and can be treated as a perturbation about an effective flat surface. In our model, the wavelength of the roughness is very small compared to the amplitude. Thus, the surface is considered very rough as its slope is large. Hence, it cannot be treated as a perturbation about a flat surface. Taken together, the two studies capture the two limits of surface roughness.

(ii) Mohammadi et al. [46] use a perturbation method for homogenization treating the amplitude as a perturbation parameter. They obtain a homogenized system consisting of a flat surface with effective surface stress and effective surface elasticity. In our work, we employ a multi-scale homogenization method which replaces the highly rough surface with an equivalent layer or film of finite thickness with effective bulk elasticity moduli.

(iii) Since the model proposed by Mohammadi et al. [46] is based on the Gurtin–Murdoch theory, the effective flat surface obtained by them does not possess curvature-dependence of the surface energy. Our model, based on multi-scale homogenization, furnishes a natural way to draw connection with the Steigmann–Ogden theory to provide estimates for curvature-dependent surface energy constants. This is possible because our homogenized system replaces the rough surface with an effective layer of finite thickness which inherently possesses bending rigidity even though we do not consider curvature-dependent surface energy to begin with.

(iv) Although highly rough surfaces have received little attention, there a few notable exceptions [48–51]. However, like Ref. [47], all these studies use the multi-scale homogenization approach to study highly rough interfaces without considering interfacial energy. In contrast, we specifically study the homogenization of highly rough surfaces endowed with surface elasticity.

The outline of the rest of the paper is as follows. Section 2 sets the general mathematical framework for incorporating surface elasticity theory and formulates the homogenization problem. Section 3 describes our multiscale homogenization scheme. In Sec. 4, we derive the effective elastic properties and the effective equations of equilibrium in the homogenized layer. Section 5 presents our explicit calculations for the case of a sinusoidal roughness. We specialize our results to a case of a thin film of finite thickness with a highly rough surface. The discussion includes a comparison of our results with those of Nevard and Keller [47] and Mohammadi et al. [46]. Our results and concluding remarks are summarized in Sec. 6.

2 General Framework and Problem Formulation

2.1 Useful Notations. Let $\mathrm{B} \subset \mathbb{R}^3$ be a regular simply connected domain, $\hat{\mathbf{n}}$ be the unit outward normal on $\partial\mathrm{B}$ at a point P, and $\mathbf{I}$ be the identity mapping from $\mathbb{R}^3$ to $\mathbb{R}^3$. Then, the surface projection tensor $\mathbb{P}$ from $\mathbb{R}^3$ to the tangent surface $\Gamma = \{\mathbf{a} \in \mathbb{R}^3 : \mathbf{a} \cdot \hat{\mathbf{n}} = 0\}$ at point P on $\partial\mathrm{B}$ is defined as,

$$\mathbb{P} = \mathbf{I} - \hat{\mathbf{n}} \otimes \hat{\mathbf{n}} \tag{1}$$

Let $\mathbf{v}$ and $\mathbf{T}$ be smooth vector and second-order tensor fields, respectively. Their projection on a smooth surface with outward normal $\hat{\mathbf{n}}$ is given by

$$\mathbf{v}_s = \mathbb{P}\mathbf{v} \quad \text{and} \quad \mathbf{T}_s = \mathbb{P}\mathbf{T}\mathbb{P} \tag{2}$$

Let $\phi : \mathrm{B} \to \mathbb{R}$ be a smooth scalar field and $\mathbf{v} : \mathrm{B} \to \mathbb{R}^3$ be a smooth vector field. Then, using Eq. (1), the surface gradients of these fields are defined as

$$\nabla_s \phi = \mathbb{P}\nabla\phi, \quad \text{and} \quad \nabla_s \mathbf{v} = (\nabla \mathbf{v})\mathbb{P} \tag{3}$$

In addition, the surface divergence of a vector field $\mathbf{v}$ and tensor field $\mathbf{T}$ are defined as

$$\mathrm{div}_s\mathbf{v} = \mathrm{tr}(\nabla_s\mathbf{v}), \quad \text{and} \quad \mathbf{a}\cdot\mathrm{div}_s\mathbf{T} = \mathrm{div}_s(\mathbf{T}^T\mathbf{a}) \tag{4}$$

where "tr" denotes the trace and $\mathbf{a}\in\mathbb{R}^3$ is an arbitrary constant vector.

2.2 Surface Elasticity. Consider a linear elastic body occupying a regular domain $\mathrm{B}\subset\mathbb{R}^3$ and let $\mathbf{C}:\mathbb{R}^{3\times3}\to\mathbb{R}^{3\times3}$ be a fourth-order stiffness tensor. In the absence of body forces, the displacement $\mathbf{u}:\mathrm{B}\to\mathbb{R}^3$ satisfies the following equilibrium equation of linear elasticity,

$$\mathrm{div}(\mathbf{C}\nabla\mathbf{u}) = 0 \quad \text{in B} \tag{5}$$

To specify the boundary conditions on the surface, we take recourse in the linearized surface elasticity theory [30,31]. Treating the surface as a deformable elastic membrane attached to the bulk without slipping, the surface stress $\mathbf{S}_s$ is given by

$$\mathbf{S}_s = \mathbf{C}_s\nabla\mathbf{u} + \mathbf{S}_s^0 \quad \text{on } \partial\mathrm{B} \tag{6}$$

where $\mathbf{S}_s^0 = \tau^0\mathbf{I}_s$ is the isotropic residual surface stress tensor and τ^0 is its magnitude. $\mathbf{I}_s$ is called the surface identity tensor which is the projection of the identity tensor on the surface calculated using Eq. (2). $\mathbf{C}_s:\mathbb{R}^{3\times3}\to\mathbb{R}^{3\times3}$ is the fourth-order surface stiffness tensor that can be defined as

$$\mathbf{C}_s(\boldsymbol{\epsilon}_s) = 2\mu^s\boldsymbol{\epsilon}_s + \lambda^s\mathrm{Tr}(\boldsymbol{\epsilon}_s)\mathbf{I}_s, \quad \forall\ \boldsymbol{\epsilon}_s\in\mathbb{R}^{3\times3}. \tag{7}$$

μ^s and λ^s are the surface elastic properties analogous to the bulk Lamé constants. ϵ_s is the infinitesimal surface strain and is defined as

$$\boldsymbol{\epsilon}_s = \mathbb{P}\boldsymbol{\epsilon}\mathbb{P} = \frac{1}{2}[\mathbb{P}\nabla_s\mathbf{u} + (\mathbb{P}\nabla_s\mathbf{u})^T] \tag{8}$$

Following Mohammadi et al. [46], we obtain the boundary condition as

$$(\mathbf{C}\nabla\mathbf{u})\hat{\mathbf{n}} = \mathrm{div}_s(\mathbf{C}_s\nabla\mathbf{u} + \mathbf{S}_s^0) \quad \text{on } \partial\mathrm{B} \tag{9}$$

It is important to bear in mind that the reference configuration taken here is the initial configuration. Since the equations are derived in the reference configuration, $\mathbf{S} = \mathbf{C}\nabla\mathbf{u}$ is the first Piola–Kirchhoff bulk stress tensor and $\mathbf{S}_s$ defined in Eq. (6) is the first Piola–Kirchhoff surface stress tensor. In linearized elasticity, the different measures of stress are equivalent in the absence of residual stresses. However, in the presence of surface stress, which is a residual stress present even in the reference configuration, the equivalence of the different stress measures—first Piola-Kirchhoff, second Piola-Kirchhoff, and Cauchy stress tensors—no longer holds (see [32,52]). The Cauchy surface stress tensor is then given by

$$\boldsymbol{\sigma}_s = [\det(\mathbf{I}_s + \nabla_s\mathbf{u})]^{-1}\,\mathbf{S}_s(\mathbf{I}_s + \nabla_s\mathbf{u})^{\mathrm{T}} \tag{10}$$

2.3 Problem Formulation. As depicted in Fig. 1(*a*), we consider a linear elastic body that occupies a three-dimensional domain $\mathrm{B} = \{(x_1, x_2, x_3) : x_3 < f(x_1, x_2)\}$ where $f(x_1, x_2)$ denotes a very rough surface in the reference configuration. Thus, $f(x_1, x_2)$ varies rapidly with a large amplitude δ, and a small wavelength ε, i.e., $\delta \gg \varepsilon$. Then, our original boundary value problem is given by Eqs. (5) and (9):

$$\begin{cases} \mathrm{div}(\mathbf{C}\nabla\mathbf{u}) = 0 \quad \text{in B}, \\ (\mathbf{C}\nabla\mathbf{u})\hat{\mathbf{n}} = \mathrm{div}_s(\mathbf{C}_s\nabla\mathbf{u} + \mathbf{S}_s^0) \quad \text{on } \partial\mathrm{B} \end{cases} \tag{11}$$

The objective of this work is to use multi-scale homogenization to reduce the original problem to an equivalent boundary value problem of the following form and illustrated by Fig. 1(*b*):

$$\begin{cases} \mathrm{div}(\mathbf{C}\nabla\mathbf{u}) = 0 \quad \text{in } \mathrm{B}_1, \\ \mathrm{div}(\mathbf{C}^{eff}\nabla\mathbf{u}) + \mathbf{f} = 0 \quad \text{in } \mathrm{B}_2 \end{cases} \tag{12}$$

System (12) describes the boundary value problem of a linear elastic composite body consisting of regions B_1 and B_2. Region B_2 denotes the upper layer of thickness δ corresponding to the amplitude of the rough surface, and is governed by the effective equilibrium equation $(12)_2$ with $\mathbf{C}^{eff}$ and $\mathbf{f}$ being the effective elastic moduli and forcing term respectively. B_1 corresponds to the bulk which obeys the original equilibrium equation established in (5).

3 Multiscale Homogenization Approach

We follow the multiscale homogenization method proposed by Nevard and Keller [47]. They use it to solve a general boundary value problem in three-dimensions with a very rough interface separating two linear elastic bodies. The explicit solution for the homogenization problem entails solving the boundary value problem over a periodic cell, also known as the "unit cell problem." To solve the unit cell problem in our case, we follow the notation of Vinh and Tung [48]. They use the multi-scale homogenization approach of Ref. [47] to derive explicit results for a two-dimensional elastic domain with a very rough interface. We also reduce the problem to two dimensions as it not only makes it amenable to explicit calculations, but it also covers a variety of practical problems that can be represented by two dimensional domains, such as biological membranes and thin films. To this end, we consider our domain B to be a half-plane with a very rough surface defined as $\partial\mathrm{B} = \{(x_1, x_3) : x_3 = \overline{f}(x_1)\}$. The function $\overline{f}(x_1)$ has a small period ε and oscillates between $x_3 = -(\delta/2)$ and $x_3 = \delta/2$ with $\varepsilon/\delta \ll 1$. We require $\overline{f}(x_1)$ to be periodic in x_1 (see Fig. 2).

3.1 Introduction of Separation of Scales. The central ansatz underlying multiscale homogenization is that the wavelength ε of the surface roughness is very small compared to other relevant lengths, specifically the amplitude δ of the surface profile. In

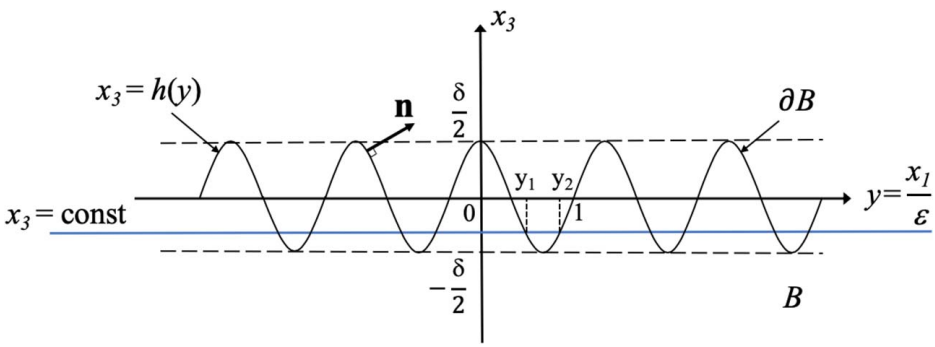

Fig. 2 The surface $\partial\mathrm{B}$ in the yx_3 domain where y varies from 0 to 1. y_1 and y_2 are two root of the equation $f(y) =$ constant in the interval [0, 1]. n denotes the normal.

other words, as $\varepsilon \to 0$, we have a very rough surface as its slope is very large. This inherent separation of scales is made explicit by defining y such that $y = x_1/\varepsilon$ [53]. Thus, y is a fast variable and x_1 is the macroscopic or slow variable. As illustrated in Fig. 2, let $f(y) = \overline{f}(\varepsilon y)$ be the mathematical function describing the surface profile in terms of the fast variable y. Thus, $f(y)$ is a periodic function with period 1 and amplitude δ. We assume that the equation $x_3 = f(y) =$ constant has exactly two roots, y_1 and y_2 in the interval [0,1]. The outward unit normal to the boundary $\partial B = \{x_3 = \overline{f}(x_1)\}$ is expressed as

$$\hat{\mathbf{n}} = \frac{1}{\sqrt{1 + \varepsilon^{-2} f_y^2}} \begin{bmatrix} -\varepsilon^{-1} f_y \\ 1 \end{bmatrix} = \frac{\mathbf{n}}{\|\mathbf{n}\|} \tag{13}$$

where $f_y = df/dy$ and $\|\mathbf{n}\| = \sqrt{1 + \varepsilon^{-2} f_y^2}$ is the magnitude of the outward normal vector, $\mathbf{n}$.

To make the dependence of $f(y)$ on δ explicit, we define $f(y) = \delta f_0(y)$. Note that since δ is the amplitude, $f_0(y)$ is simply a periodic function describing the roughness profile. $f_0(y)$ is a continuously differentiable albeit arbitrary functions of y. Now, using the large amplitude, small wavelength approximation, $\varepsilon/\delta \ll 1$, the Taylor expansion of $\|\mathbf{n}\|$ yields,

$$\|\mathbf{n}\| = \varepsilon^{-1} f_y \sqrt{1 + \frac{\varepsilon^2}{\delta^2} \frac{1}{f_{0y}^2}} = \varepsilon^{-1} f_y + \frac{1}{2} \frac{\varepsilon}{f_y} - \frac{1}{8} \frac{\varepsilon^3}{f_y^3} + o\left(\frac{\varepsilon^5}{\delta^5}\right) \tag{14}$$

Similarly, using the expression for $\hat{\mathbf{n}}$ in Eq. (1), the projection tensor is obtained as,

$$\mathbb{P} = \mathbf{I} - \frac{\mathbf{n}}{\|\mathbf{n}\|} \otimes \frac{\mathbf{n}}{\|\mathbf{n}\|} \simeq \begin{bmatrix} \frac{\varepsilon^2}{f_y^2} & \frac{\varepsilon}{f_y} - \frac{\varepsilon^3}{f_y^3} \\ \frac{\varepsilon}{f_y} - \frac{\varepsilon^3}{f_y^3} & 1 - \frac{\varepsilon^2}{f_y^2} \end{bmatrix} + o\left(\frac{\varepsilon^3}{\delta^3}\right) \tag{15}$$

where we again invoke the $\varepsilon/\delta \ll 1$ approximation and use the Taylor expansion.

Our goal is to determine the displacement $\mathbf{u}(x_1, x_3, \varepsilon)$ for small values of ε. The in-plane component u_2 as well as the dependence on x_2 are neglected, since we are working with a two-dimensional domain. The displacement $\mathbf{u}$ satisfies the equilibrium equation and the boundary condition in Eq. (11). Following [47], we define

$$\mathbf{U}(x_1, x_3, y, \varepsilon) = \mathbf{u}(x_1, x_3, \varepsilon) \tag{16}$$

to make the dependence on the fast variable explicit. Then,

$$\mathbf{u}_{,1} = \mathbf{U}_{,1} + \varepsilon^{-1} \mathbf{U}_{,y} \text{ and } \mathbf{u}_{,3} = \mathbf{U}_{,3} \tag{17}$$

where $\phi_{,1} = \partial\phi/\partial x_1$, $\phi_{,3} = \partial\phi/\partial x_3$, and $\phi_{,y} = \partial\phi/\partial y$ for a scalar function $\phi(x_1, x_3, y)$. To express the boundary value problem (11) in terms of $\mathbf{U}(x_1, x_3, y, \varepsilon)$, we employ the notation used by [48] for our subsequent calculations. Assuming isotropic linear elastic material, the equilibrium equation $(11)_1$ yields a system of equations that can be written in the following compact form [48,54].

$$\mathbf{A}_{hk} \mathbf{u}_{,kh} = 0, \quad h, k = 1, 3 \tag{18}$$

where $\mathbf{u} = [u_1 \quad u_3]^T$ and the $\mathbf{A}$ matrices are as follows:

$$\begin{aligned} \mathbf{A}_{11} &= \begin{bmatrix} C_{1111} & C_{1131} \\ C_{3111} & C_{3131} \end{bmatrix} = \begin{bmatrix} \lambda + 2\mu & 0 \\ 0 & \mu \end{bmatrix} \quad \mathbf{A}_{13} = \begin{bmatrix} C_{1113} & C_{1133} \\ C_{3113} & C_{3133} \end{bmatrix} = \begin{bmatrix} 0 & \lambda \\ \mu & 0 \end{bmatrix} \\ \mathbf{A}_{31} &= \begin{bmatrix} C_{1311} & C_{1331} \\ C_{3311} & C_{3331} \end{bmatrix} = \begin{bmatrix} 0 & \mu \\ \lambda & 0 \end{bmatrix} \quad \mathbf{A}_{33} = \begin{bmatrix} C_{1313} & C_{1333} \\ C_{3313} & C_{3333} \end{bmatrix} = \begin{bmatrix} \mu & 0 \\ 0 & \lambda + 2\mu \end{bmatrix} \end{aligned} \tag{19}$$

Note that since the Lamé constants, λ and μ, are positive, the $\mathbf{A}$ matrices are invertible. In order to express the boundary condition $(11)_2$ in explicit notation, we first multiply both sides with $\|\mathbf{n}\|$ to get

$$(\mathbf{C}\nabla\mathbf{u})\mathbf{n} = \|\mathbf{n}\| \text{div}_s(\mathbf{C}_s \nabla\mathbf{u} + \mathbf{S}_s^0) \tag{20}$$

In terms of the matrices introduced in Eq. (19), the left-hand side of Eq. (20) becomes,

$$(\mathbf{A}_{hk}\mathbf{u}_{,k})\mathbf{n}_h = -\varepsilon^{-1} f_y (\mathbf{A}_{11}\mathbf{u}_{,1} + \mathbf{A}_{13}\mathbf{u}_{,3}) + \mathbf{A}_{31}\mathbf{u}_{,1} + \mathbf{A}_{33}\mathbf{u}_{,3} \tag{21}$$

while the right-hand side of Eq. (20) can be expressed in the following compact form,

$$\|\mathbf{n}\| \text{div}_s(\mathbf{C}_s \nabla\mathbf{u} + \mathbf{S}_s^0) = \mathbf{B}_{hk}\mathbf{u}_{,hk} + \mathbf{D}_j \mathbf{u}_{,j} + \mathbf{T}, \quad h, k = 1, 3 \tag{22}$$

The expressions for $\mathbf{B}$, $\mathbf{D}$ and $\mathbf{T}$ matrices (keeping only the orders that will contribute to the BVPs up to ε^2) are given in Appendix A. After substituting Eqs. (16) and (17) in Eqs. (18), (21), and (22), and some tedious calculations, we can express the equilibrium equation (18) and the boundary condition (20) in terms of $\mathbf{U}(x_1, x_3, y, \varepsilon)$ (see Appendix A for details).

3.2 Asympotic Expansion. We now assume that the displacement $\mathbf{U}(x_1, x_3, y)$ can be expressed for small values of the wavelength ε as an asymptotic expansion,

$$\mathbf{U}(x_1, x_3, y, \varepsilon) = \mathbf{u}^{(0)}(x_1, x_3) + \varepsilon \mathbf{u}^{(1)}(x_1, x_3, y) + \varepsilon^2 \mathbf{u}^{(2)}(x_1, x_3, y) + O(\varepsilon^2) \tag{23}$$

Note that $\mathbf{u}^{(0)}(x_1, x_3)$ does not depend on the slow variable y. In fact, it is the macroscopic displacement that is observed at length scales larger than that of the surface roughness. Since $\mathbf{U}$ is periodic in y, it follows that $\mathbf{u}^{(1)}$, and $\mathbf{u}^{(2)}$ are periodic in y with period 1. We now substitute the asymptotic expansion of the displacement in the boundary value problem derived after introduction of the separation of scales (Appendix A) to express the equilibrium equation and boundary condition in terms of $\mathbf{u}^{(0)}$, $\mathbf{u}^{(1)}$, and $\mathbf{u}^{(2)}$.

3.3 Boundary Value Problems for Perturbed Solution. The equilibrium equation and surface equation obtained after incorporating the asymptotic expansion (23) include terms with different orders of ε. Gathering the coefficients of the same power of ε yields the following set of boundary value problems.

Order ε^{-1}:

$$\begin{cases} [\mathbf{A}_{11}\mathbf{u}_{,y}^{(1)} + \mathbf{A}_{11}\mathbf{u}_{,1}^{(0)} + \mathbf{A}_{13}\mathbf{u}_{,3}^{(0)}]_{,y} = 0, & x_3 < f(y) \\ f_y(-\mathbf{A}_{11}\mathbf{u}_{,y}^{(1)} - \mathbf{A}_{11}\mathbf{u}_{,1}^{(0)} - \mathbf{A}_{13}\mathbf{u}_{,3}^{(0)}) = \mathbf{B}_{33}^{(-1)}\mathbf{u}_{,33}^{(0)} + \dfrac{f_{yy}}{f_y}\mathbf{D}_3^{(-1)}\mathbf{u}_{,3}^{(0)} + \dfrac{f_{yy}}{f_y}\mathbf{T}^{(-1)}, & x_3 = f(y) \end{cases} \tag{24}$$

Order ε^0:

$$\begin{cases} [\mathbf{A}_{11}\mathbf{u}^{(0)}_{,1} + \mathbf{A}_{13}\mathbf{u}^{(0)}_{,3} + \mathbf{A}_{11}\mathbf{u}^{(1)}_{,y}]_{,1} + [\mathbf{A}_{31}\mathbf{u}^{(0)}_{,1} + \mathbf{A}_{33}\mathbf{u}^{(0)}_{,3} + \mathbf{A}_{31}\mathbf{u}^{(1)}_{,y}]_{,3} + [\mathbf{A}_{11}\mathbf{u}^{(2)}_{,y} + \mathbf{A}_{11}\mathbf{u}^{(1)}_{,1} + \mathbf{A}_{13}\mathbf{u}^{(1)}_{,3}]_{,y} = 0, \;\; x_3 < f(y) \\ -f_y\mathbf{A}_{11}\mathbf{u}^{(2)}_{y} - f_y\mathbf{A}_{11}\mathbf{u}^{(1)}_{,1} - f_y\mathbf{A}_{13}\mathbf{u}^{(1)}_{,3} + \mathbf{A}_{31}\mathbf{u}^{(1)}_{,y} + \mathbf{A}_{31}\mathbf{u}^{(0)}_{,1} + \mathbf{A}_{33}\mathbf{u}^{(0)}_{,3} = f_y\mathbf{B}^{(-1)}_{33}\mathbf{u}^{(1)}_{,33} + \mathbf{B}^{(0)}_{13}\mathbf{u}^{(0)}_{,13} + \mathbf{B}^{(0)}_{31}\mathbf{u}^{(0)}_{,31} + \mathbf{B}^{(0)}_{33}\mathbf{u}^{(0)}_{,33} + \mathbf{B}^{(0)}_{13}\mathbf{u}^{(1)}_{,y3} + \mathbf{B}^{(0)}_{31}\mathbf{u}^{(1)}_{,3y} \\ + \frac{\mathbf{B}^{(1)}_{11}}{f_y}\mathbf{u}^{(1)}_{,yy} + \frac{f_{yy}}{f_y^2}(\mathbf{T}^{(0)} + \mathbf{D}^{(0)}_1\mathbf{u}^{(0)}_{,1} + \mathbf{D}^{(0)}_3\mathbf{u}^{(0)}_{,3} + \mathbf{D}^{(0)}_1\mathbf{u}^{(1)}_{,y}) + \frac{f_{yy}}{f_y}\mathbf{D}^{(-1)}_3\mathbf{u}^{(1)}_{,3}, \;\; x_3 = f(y) \end{cases} \tag{25}$$

Order ε^1:

$$\begin{cases} [\mathbf{A}_{11}\mathbf{u}^{(1)}_{,1} + \mathbf{A}_{13}\mathbf{u}^{(1)}_{,3} + \mathbf{A}_{11}\mathbf{u}^{(2)}_{,y}]_{,1} + [\mathbf{A}_{31}\mathbf{u}^{(1)}_{,1} + \mathbf{A}_{31}\mathbf{u}^{(2)}_{,y} + \mathbf{A}_{33}\mathbf{u}^{(1)}_{,3}]_{,3} + [\mathbf{A}_{11}\mathbf{u}^{(2)}_{,1} + \mathbf{A}_{13}\mathbf{u}^{(2)}_{,3}]_{,y} = 0, \;\; x_3 < f(y) \\ -f_y\mathbf{A}_{11}\mathbf{u}^{(2)}_{,1} - f_y\mathbf{A}_{13}\mathbf{u}^{(2)}_{,3} + \mathbf{A}_{31}\mathbf{u}^{(2)}_{,y} + \mathbf{A}_{31}\mathbf{u}^{(1)}_{,1} + \mathbf{A}_{33}\mathbf{u}^{(1)}_{,3} = \frac{\mathbf{B}^{(2)}_{11}}{f_y^2}\mathbf{u}^{(1)}_{,yy} + \frac{\mathbf{B}^{(1)}_{11}}{f_y}\mathbf{u}^{(0)}_{,11} + \frac{\mathbf{B}^{(1)}_{13}}{f_y}\mathbf{u}^{(0)}_{,13} + \frac{\mathbf{B}^{(1)}_{31}}{f_y}\mathbf{u}^{(0)}_{,31} + \frac{\mathbf{B}^{(1)}_{33}}{f_y}\mathbf{u}^{(0)}_{,33} + \frac{\mathbf{B}^{(1)}_{11}}{f_y}(\mathbf{u}^{(1)}_{,1y} + \mathbf{u}^{(1)}_{,y1}) + \frac{\mathbf{B}^{(1)}_{13}}{f_y}\mathbf{u}^{(1)}_{,y3} \\ + \frac{\mathbf{B}^{(1)}_{31}}{f_y}\mathbf{u}^{(1)}_{,3y} + \frac{\mathbf{B}^{(1)}_{11}}{f_y}\mathbf{u}^{(2)}_{,yy} + \mathbf{B}^{(0)}_{13}\mathbf{u}^{(1)}_{,13} + \mathbf{B}^{(0)}_{31}\mathbf{u}^{(1)}_{,31} + \mathbf{B}^{(0)}_{33}\mathbf{u}^{(1)}_{,33} + \mathbf{B}^{(0)}_{13}\mathbf{u}^{(2)}_{,y3} + \mathbf{B}^{(0)}_{31}\mathbf{u}^{(2)}_{,3y} + f_y\mathbf{B}^{(-1)}\mathbf{u}^{(2)}_{,33} + \frac{f_{yy}}{f_y^3}(\mathbf{D}^{(1)}_1\mathbf{u}^{(0)}_{,1} + \mathbf{D}^{(1)}_3\mathbf{u}^{(0)}_{,3} \\ + \mathbf{D}^{(1)}_1\mathbf{u}^{(1)}_{,y} + \mathbf{T}^{(1)}) + \frac{f_{yy}}{f_y^2}(\mathbf{D}^{(0)}_1\mathbf{u}^{(1)}_{,1} + \mathbf{D}^{(0)}_3\mathbf{u}^{(1)}_{,3} + \mathbf{D}^{(0)}_1\mathbf{u}^{(2)}_{,y}) + \frac{f_{yy}}{f_y}\mathbf{D}^{(-1)}_3\mathbf{u}^{(2)}_{,3}, \;\; x_3 = f(y) \end{cases} \tag{26}$$

Order ε^2:

$$\begin{cases} \mathbf{A}_{11}\mathbf{u}^{(2)}_{,11} + \mathbf{A}_{13}\mathbf{u}^{(2)}_{,31} + \mathbf{A}_{31}\mathbf{u}^{(2)}_{,13} + \mathbf{A}_{33}\mathbf{u}^{(2)}_{,33} = 0, \;\; x_3 < f(y) \\ \mathbf{A}_{31}\mathbf{u}^{(2)}_{,1} + \mathbf{A}_{33}\mathbf{u}^{(2)}_{,3} = \mathbf{B}^{(0)}_{13}\mathbf{u}^{(2)}_{,13} + \mathbf{B}^{(0)}_{31}\mathbf{u}^{(2)}_{,31} + \mathbf{B}^{(0)}_{33}\mathbf{u}^{(2)}_{,33} + \frac{\mathbf{B}^{(1)}_{11}}{f_y}\mathbf{u}^{(1)}_{,11} + \frac{\mathbf{B}^{(1)}_{13}}{f_y}\mathbf{u}^{(1)}_{,13} + \frac{\mathbf{B}^{(1)}_{31}}{f_y}\mathbf{u}^{(1)}_{,31} + \frac{\mathbf{B}^{(1)}_{33}}{f_y}\mathbf{u}^{(1)}_{,33} \\ + \frac{\mathbf{B}^{(1)}_{11}}{f_y}(\mathbf{u}^{(2)}_{,1y} + \mathbf{u}^{(2)}_{,y1}) + \frac{\mathbf{B}^{(1)}_{13}}{f_y}\mathbf{u}^{(2)}_{,y3} + \frac{\mathbf{B}^{(1)}_{31}}{f_y}\mathbf{u}^{(2)}_{,3y} + \frac{\mathbf{B}^{(2)}_{11}}{f_y^2}\mathbf{u}^{(0)}_{,11} + \frac{\mathbf{B}^{(2)}_{13}}{f_y^2}\mathbf{u}^{(0)}_{,13} + \frac{\mathbf{B}^{(2)}_{31}}{f_y^2}\mathbf{u}^{(0)}_{,31} + \frac{\mathbf{B}^{(2)}_{33}}{f_y^2}\mathbf{u}^{(0)}_{,33} + \frac{\mathbf{B}^{(2)}_{11}}{f_y^2}(\mathbf{u}^{(1)}_{,1y} \\ + \mathbf{u}^{(1)}_{,y1}) + \frac{\mathbf{B}^{(2)}_{13}}{f_y^2}\mathbf{u}^{(1)}_{,y3} + \frac{\mathbf{B}^{(2)}_{31}}{f_y^2}\mathbf{u}^{(1)}_{,3y} + \frac{\mathbf{B}^{(2)}_{11}}{f_y^2}\mathbf{u}^{(2)}_{,yy} + \frac{\mathbf{B}^{(3)}_{11}}{f_y^3}\mathbf{u}^{(1)}_{,yy} + \frac{f_{yy}}{f_y^4}(\mathbf{D}^{(2)}_1\mathbf{u}^{(0)}_{,1} + \mathbf{D}^{(2)}_3\mathbf{u}^{(0)}_{,3} + \mathbf{D}^{(2)}_1\mathbf{u}^{(1)}_{,y} + \mathbf{T}^{(2)}) \\ + \frac{f_{yy}}{f_y^3}(\mathbf{D}^{(1)}_1\mathbf{u}^{(1)}_{,1} + \mathbf{D}^{(1)}_3\mathbf{u}^{(1)}_{,3} + \mathbf{D}^{(1)}_1\mathbf{u}^{(2)}_{,y}) + \frac{f_{yy}}{f_y^2}(\mathbf{D}^{(0)}_1\mathbf{u}^{(2)}_{,1} + \mathbf{D}^{(0)}_3\mathbf{u}^{(2)}_{,3}), \;\; x_3 = f(y) \end{cases} \tag{27}$$

4 Homogenized Equations and Effective Properties

Based on the boundary value problem (25) for the order ε^0, we wish to derive homogenized equilibrium equations in terms of only the macroscopic displacement $\mathbf{u}^{(0)}(x_1, x_3)$. To this end, we first seek to express the derivatives of $\mathbf{u}^{(1)}$ and $\mathbf{u}^{(2)}$ that appear in Eq. (25) in terms of $\mathbf{u}^{(0)}$. Based on boundary value problem (24) for the order ε^{-1}, we suggest the following form for $\mathbf{u}^{(1)}$ [48],

$$\mathbf{u}^{(1)} = \mathbf{N}^1\mathbf{u}^{(0)} + \mathbf{N}^{11}\mathbf{u}^{(0)}_{,1} + \mathbf{N}^{13}\mathbf{u}^{(0)}_{,3} + \mathbf{N}^{133}\mathbf{u}^{(0)}_{,33} + \mathbf{N}^0 \tag{28}$$

where $\mathbf{N}^1$, $\mathbf{N}^{11}$, $\mathbf{N}^{13}$, $\mathbf{N}^{133}$, and $\mathbf{N}^0$ are 2×2 matrices that are functions of x_3 and y and are periodic in y with a period of 1. Substituting Eq. (28) in (24) and gathering the coefficients of $\mathbf{u}^{(0)}$, $\mathbf{u}^{(0)}_{,1}$, $\mathbf{u}^{(0)}_{,3}$, and $\mathbf{u}^{(0)}_{,33}$ and the remaining constants, we get the following systems of equations:

$$\begin{cases} (\mathbf{A}_{11}\mathbf{N}^1_{,y})_{,y} = 0, \;\; x_3 < f(y) \\ -f_y\mathbf{A}_{11}\mathbf{N}^1_{,y} = 0, \;\; x_3 = f(y) \end{cases} \tag{29}$$

$$\begin{cases} (\mathbf{A}_{11}\mathbf{N}^{11}_{,y} + \mathbf{A}_{11})_{,y} = 0, \;\; x_3 < f(y) \\ \mathbf{A}_{11}\mathbf{N}^{11}_{,y} + \mathbf{A}_{11} = 0, \;\; x_3 = f(y) \end{cases} \tag{30}$$

$$\begin{cases} (\mathbf{A}_{11}\mathbf{N}^{13}_{,y} + \mathbf{A}_{13})_{,y} = 0, \;\; x_3 < f(y) \\ -f_y(\mathbf{A}_{11}\mathbf{N}^{13}_{,y} + \mathbf{A}_{13}) = \frac{f_{yy}}{f_y}\mathbf{D}^{(-1)}_3, \;\; x_3 = f(y) \end{cases} \tag{31}$$

$$\begin{cases} (\mathbf{A}_{11}\mathbf{N}^{133}_{,y})_{,y} = 0, \;\; x_3 < f(y) \\ -f_y\mathbf{A}_{11}\mathbf{N}^{133}_{,y} = f_y\mathbf{B}^{(-1)}_{33}, \;\; x_3 = f(y) \end{cases} \tag{32}$$

$$\begin{cases} (\mathbf{A}_{11}\mathbf{N}^0_{,y})_{,y} = 0, \;\; x_3 < f(y) \\ -f_y\mathbf{A}_{11}\mathbf{N}^0_{,y} = \frac{f_{yy}}{f_y}\mathbf{T}^{(-1)}, \;\; x_3 = f(y) \end{cases} \tag{33}$$

Solving these equations yields the following expressions for the derivatives of the $\mathbf{N}$ matrices,

$$\mathbf{N}^1_{,y} = 0, \;\; x_3 \le f(y) \tag{34}$$

$$\mathbf{N}^{11}_{,y} = \begin{cases} 0, & x_3 < f(y) \\ -\mathbf{I}, & x_3 = f(y) \end{cases} \tag{35}$$

$$\mathbf{N}^{13}_{,y} = \begin{cases} \mathbf{A}^{-1}_{11} < \mathbf{A}^{-1}_{11} >^{-1} < \mathbf{A}^{-1}_{11}\mathbf{A}_{13} > - \mathbf{A}^{-1}_{11}\mathbf{A}_{13}, & x_3 < f(y) \\ -\mathbf{A}^{-1}_{11}\mathbf{A}_{13} - \mathbf{A}^{-1}_{11}\mathbf{D}^{(-1)}_3\frac{f_{yy}}{f_y^2}\Big|_{y_1}, & y = y_1 \\ -\mathbf{A}^{-1}_{11}\mathbf{A}_{13} - \mathbf{A}^{-1}_{11}\mathbf{D}^{(-1)}_3\frac{f_{yy}}{f_y^2}\Big|_{y_2}, & y = y_2 \end{cases} \tag{36}$$

$$\mathbf{N}^{133}_{,y} = \begin{cases} 0, & x_3 < f(y) \\ -\mathbf{A}^{-1}_{11}\mathbf{B}^{(-1)}_{33}, & x_3 = f(y) \end{cases} \tag{37}$$

$$\mathbf{N}^0_{,y} = \begin{cases} 0, & x_3 < f(y) \\ -\mathbf{A}^{-1}_{11}\mathbf{T}^{(-1)}\frac{f_{yy}}{f_y^2}\Big|_{y_1}, & y = y_1 \\ -\mathbf{A}^{-1}_{11}\mathbf{T}^{(0)}\frac{f_{yy}}{f_y^2}\Big|_{y_2}, & y = y_2 \end{cases} \tag{38}$$

where $<\phi> = \int_0^1 \phi\, dy = \int_0^{y_1} \phi\, dy + \int_{y_2}^1 \phi\, dy = (1 - y_2 + y_1)\phi$ for a constant scalar function ϕ.

We now integrate the equilibrium equation $(25)_1$ with respect to y over [0, 1] for a constant x_3 [47]. To perform this integration, we first define y_1 and y_2 as the roots of the equation $x_3 = h(y)$ at a

constant x_3 (see Fig. 2).

$$\int_0^1 ([\mathbf{A}_{11}\mathbf{u}_{,1}^{(0)} + \mathbf{A}_{13}\mathbf{u}_{,3}^{(0)} + \mathbf{A}_{11}\mathbf{u}_{,y}^{(1)}]_{,1} + [\mathbf{A}_{31}\mathbf{u}_{,1}^{(0)} + \mathbf{A}_{33}\mathbf{u}_{,3}^{(0)} + \mathbf{A}_{31}\mathbf{u}_{,y}^{(1)}]_{,3} + [\mathbf{A}_{11}\mathbf{u}_{,y}^{(2)} + \mathbf{A}_{11}\mathbf{u}_{,1}^{(1)} + \mathbf{A}_{13}\mathbf{u}_{,3}^{(1)}]_{,y})\, dy = 0 \tag{39}$$

For convenience, we define

$$e_1 = \int_0^1 [\mathbf{A}_{11}\mathbf{u}_{,1}^{(0)} + \mathbf{A}_{13}\mathbf{u}_{,3}^{(0)} + \mathbf{A}_{11}\mathbf{u}_{,y}^{(1)}]_{,1}\, dy$$

$$e_2 = \int_0^1 [\mathbf{A}_{31}\mathbf{u}_{,1}^{(0)} + \mathbf{A}_{33}\mathbf{u}_{,3}^{(0)} + \mathbf{A}_{31}\mathbf{u}_{,y}^{(1)}]_{,3}\, dy$$

$$e_3 = \int_0^1 [\mathbf{A}_{11}\mathbf{u}_{,y}^{(2)} + \mathbf{A}_{11}\mathbf{u}_{,1}^{(1)} + \mathbf{A}_{13}\mathbf{u}_{,3}^{(1)}]_{,y}\, dy$$

We now note that $\|\mathbf{C}\| \gg \|\mathbf{C}_s\|\varepsilon$ for typical solids where ε is the wavelength and typically on the order of 10 nm. For instance, the inequality is valid for copper since it has $\|\mathbf{C}\| \sim 10^{11}$ Pa while $\|\mathbf{C}_s\| \sim$ 1 N/m. Then, enforcing this inequality and neglecting lower order terms on the right-hand side of Eq. $(25)_2$, we get,

$$-f_y\left(\mathbf{A}_{11}\mathbf{u}_{,y}^{(2)} + \mathbf{A}_{11}\mathbf{u}_{,1}^{(1)} + \mathbf{A}_{13}\mathbf{u}_{,3}^{(1)}\right) + \mathbf{A}_{31}\mathbf{u}_{,y}^{(1)} + \mathbf{A}_{31}\mathbf{u}_{,1}^{(0)} + \mathbf{A}_{33}\mathbf{u}_{,3}^{(0)} = \mathbf{B}_{13}^{(0)}\mathbf{u}_{,13}^{(0)} + \mathbf{B}_{31}^{(0)}\mathbf{u}_{,31}^{(0)} + \mathbf{B}_{33}^{(0)}\mathbf{u}_{,33}^{(0)} + \mathbf{B}_{13}^{(0)}\mathbf{u}_{,y3}^{(1)} + \frac{f_{yy}}{f_y^2}(\mathbf{T}^{(0)} + \mathbf{D}_1^{(0)}\mathbf{u}_{,1}^{(0)} + \mathbf{D}_3^{(0)}\mathbf{u}_{,3}^{(0)}),\quad x_3 = f(y) \tag{40}$$

We can now evaluate e_3 using Eq. (40) to get,

$$e_3 = \frac{1}{f_y(y_1)}\mathbf{A}_{31}\mathbf{u}_{,y}^{(1)}\Big|_{y_1} - \frac{1}{f_y(y_2)}\mathbf{A}_{31}\mathbf{u}_{,y}^{(1)}\Big|_{y_2} + \left(\frac{1}{f_y(y_1)} - \frac{1}{f_y(y_2)}\right) \times [\mathbf{A}_{31}\mathbf{u}_{,1}^{(0)} + \mathbf{A}_{33}\mathbf{u}_{,3}^{(0)} - \mathbf{B}_{13}^{(0)}\mathbf{u}_{,13}^{(0)} + \mathbf{B}_{31}^{(0)}\mathbf{u}_{,31}^{(0)} + \mathbf{B}_{33}^{(0)}\mathbf{u}_{,33}^{(0)}] + \left(\frac{f_{yy}}{f_y^3}\Big|_{y_2} - \frac{f_{yy}}{f_y^3}\Big|_{y_1}\right)[\mathbf{D}_1^{(0)}\mathbf{u}_{,1}^{(0)} + \mathbf{D}_3^{(0)}\mathbf{u}_{,3}^{(0)} + \mathbf{T}^{(0)}] \tag{41}$$

By substituting for $\mathbf{u}_{,y}^{(1)}|_{y_i}$ in terms of the expressions (34)–(38) for the $\mathbf{N}_{,y}$ matrices we have,

$$e_3 = \left(\frac{1}{f_y(y_1)} - \frac{1}{f_y(y_2)}\right)[(\mathbf{A}_{33} - \mathbf{A}_{31}\mathbf{A}_{11}^{-1}\mathbf{A}_{13})\mathbf{u}_{,3}^{(0)} - (\mathbf{A}_{31}\mathbf{A}_{11}^{-1}\mathbf{B}_{33}^{(-1)} + \mathbf{B}_{33}^{(0)})\mathbf{u}_{,33}^{(0)} - \mathbf{B}_{13}^{(0)}\mathbf{u}_{,13}^{(0)} - \mathbf{B}_{31}^{(0)}\mathbf{u}_{,31}^{(0)}] + \left(\frac{f_{yy}}{f_y^3}\Big|_{y_2} - \frac{f_{yy}}{f_y^3}\Big|_{y_1}\right)[\mathbf{D}_1^{(0)}\mathbf{u}_{,1}^{(0)} + \mathbf{D}_3^{(0)}\mathbf{u}_{,3}^{(0)} + \mathbf{T}^{(0)}] - \left(\frac{f_{yy}}{f_y^3}\Big|_{y_1} - \frac{f_{yy}}{f_y^3}\Big|_{y_2}\right) \times [\mathbf{A}_{31}\mathbf{A}_{11}^{-1}\mathbf{D}_3^{(-1)}\mathbf{u}_{,3}^{(0)} + \mathbf{A}_{31}\mathbf{A}_{11}^{-1}\mathbf{T}^{(-1)}] \tag{42}$$

We now proceed to evaluate e_1 and e_2 as follows.

$$e_1 = \int_0^1 [\mathbf{A}_{11}\mathbf{u}_{,1}^{(0)} + \mathbf{A}_{13}\mathbf{u}_{,3}^{(0)} + \mathbf{A}_{11}(\mathbf{N}_{,y}^{11}\mathbf{u}_{,1}^{(0)} + \mathbf{N}_{,y}^{13}\mathbf{u}_{,3}^{(0)} + \mathbf{N}_{,y}^{133}\mathbf{u}_{,33}^{(0)} + \mathbf{N}_{,y}^{0})]_{,1}\, dy = \langle \mathbf{A}_{11} + \mathbf{A}_{11}\mathbf{N}_{,y}^{11}\rangle\mathbf{u}_{,11}^{(0)} + \langle \mathbf{A}_{13} + \mathbf{A}_{11}\mathbf{N}_{,y}^{13}\rangle\mathbf{u}_{,31}^{(0)} + \langle \mathbf{A}_{11}\mathbf{N}_{,y}^{133}\rangle\mathbf{u}_{,33}^{(0)} \tag{43}$$

Using Eqs. (35)–(38), the terms between angular brackets can be evaluated as

$$\langle \mathbf{A}_{11} + \mathbf{A}_{11}\mathbf{N}_{,y}^{11}\rangle = \langle \mathbf{A}_{11}\rangle \tag{44}$$

$$\langle \mathbf{A}_{13} + \mathbf{A}_{11}\mathbf{N}_{,y}^{13}\rangle = \langle \mathbf{A}_{11}^{-1}\rangle^{-1}\langle \mathbf{A}_{11}^{-1}\mathbf{A}_{13}\rangle = \mathbf{A}_{13} \tag{45}$$

$$\langle \mathbf{A}_{11}\mathbf{N}_{,y}^{133}\rangle = 0 \tag{46}$$

Similarly,

$$e_2 = \int_0^1 [\mathbf{A}_{31}\mathbf{u}_{,1}^{(0)} + \mathbf{A}_{33}\mathbf{u}_{,3}^{(0)} + \mathbf{A}_{31}(\mathbf{N}_{,y}^{11}\mathbf{u}_{,1}^{(0)} + \mathbf{N}_{,y}^{13}\mathbf{u}_{,13}^{(0)} + \mathbf{N}_{,y}^{133}\mathbf{u}_{,33}^{(0)} + \mathbf{N}_{,y}^{0})]_{,3}\, dy = [\langle \mathbf{A}_{31} + \mathbf{A}_{31}\mathbf{N}_{,y}^{11}\rangle\mathbf{u}_{,1}^{(0)}]_{,3} + [\langle \mathbf{A}_{33} + \mathbf{A}_{31}\mathbf{N}_{,y}^{13}\rangle\mathbf{u}_{,3}^{(0)}]_{,3} + [\langle \mathbf{A}_{31}\mathbf{N}_{,y}^{133}\rangle\mathbf{u}_{,33}^{(0)}]_{,3} \tag{47}$$

where the terms between angular brackets can be evaluated as

$$\langle \mathbf{A}_{31} + \mathbf{A}_{31}\mathbf{N}_{,y}^{11}\rangle = \langle \mathbf{A}_{31}\rangle \tag{48}$$

$$\langle \mathbf{A}_{33} + \mathbf{A}_{31}\mathbf{N}_{,y}^{13}\rangle = \langle \mathbf{A}_{33}\rangle \tag{49}$$

$$\langle \mathbf{A}_{31}\mathbf{N}_{,y}^{133}\rangle = 0 \tag{50}$$

Thus, we get the following equilibrium equation in terms of $\mathbf{u}^{(0)}$ which is valid in the equivalent effective layer:

$$\begin{aligned}&\langle \mathbf{A}_{11}\rangle\mathbf{u}_{,11}^{(0)} + [\mathbf{A}_{13} - (y_1' - y_2')\mathbf{B}_{31}^{(0)}]\mathbf{u}_{,31}^{(0)} + [(\langle \mathbf{A}_{31}\rangle - (y_1' - y_2')\mathbf{B}_{13}^{(0)})\mathbf{u}_{,1}^{(0)}]_{,3} \\ &+ [(\langle \mathbf{A}_{33}\rangle - (y_1' - y_2')[\mathbf{A}_{31}\mathbf{A}_{11}^{-1}\mathbf{B}_{33}^{(-1)} + \mathbf{B}_{33}^{(0)}])\mathbf{u}_{,3}^{(0)}]_{,3} \\ &+ (y_1'' - y_2'')[\mathbf{A}_{31}\mathbf{A}_{11}^{-1}\mathbf{T}^{(-1)} + \mathbf{T}^{(0)}] = (y_2'' - y_1'')[\mathbf{B}_{13}^{(0)} + \mathbf{D}_1^{(0)}]\mathbf{u}_{,1}^{(0)} \\ &+ [(y_2'' - y_1'')(\mathbf{B}_{33}^{(0)} + \mathbf{D}_3^{(0)}) + (y_2' - y_1')(\mathbf{A}_{33} \\ &- \mathbf{A}_{31}\mathbf{A}_{11}^{-1}\mathbf{A}_{13})]\mathbf{u}_{,3}^{(0)},\quad -\frac{\delta}{2} < x_3 < \frac{\delta}{2}\end{aligned} \tag{51}$$

and where we have used the following identities:

$$\frac{1}{f_y}(y_i) = \frac{dy_i}{dx_3} = y_i' \quad \text{and} \quad -\frac{f_{yy}}{f_y^3}(y_i) = \frac{d^2y_i}{dx_3^2} = y_i'',\quad i = \{1, 2\} \tag{52}$$

Introducing the separation of scales and the asymptotic expansion in the effective boundary value problem stated in Eq. (12), we can write the boundary value problem statement for $\mathbf{u}^{(0)}$ as

$$\begin{cases}\mathbf{A}_{11}\mathbf{u}_{,11}^{(0)} + \mathbf{A}_{13}\mathbf{u}_{,31}^{(0)} + \mathbf{A}_{31}\mathbf{u}_{,13}^{(0)} + \mathbf{A}_{33}\mathbf{u}_{,33}^{(0)} = 0,\quad x_3 < -\dfrac{\delta}{2} \\ \mathbf{A}_{11}^{eff}\mathbf{u}_{,11}^{(0)} + \mathbf{A}_{13}^{eff}\mathbf{u}_{,31}^{(0)} + [\mathbf{A}_{31}^{eff}\mathbf{u}_{,1}^{(0)}]_{,3} + [\mathbf{A}_{33}^{eff}\mathbf{u}_{,3}^{(0)}]_{,3} + \nabla\cdot\boldsymbol{\sigma}^* = \mathbf{D}_1^{eff}\mathbf{u}_{,1}^{(0)} + \mathbf{D}_3^{eff}\mathbf{u}_{,3}^{(0)},\quad -\frac{\delta}{2} \le x_3 \le \frac{\delta}{2}\end{cases} \tag{53}$$

Comparing Eqs. (51) and $(53)_2$ and introducing $k_s = \lambda_s + 2\mu_s$, we obtain the effective (bulk) properties in the equivalent layer $(-(\delta/2) \le x_3 \le \delta/2)$,

$$\begin{aligned}
\mathbf{A}_{11}^{eff} &= \begin{bmatrix} (\lambda+2\mu)(1-y_2+y_1) & 0 \\ 0 & \mu(1-y_2+y_1) \end{bmatrix} \\
\mathbf{A}_{13}^{eff} &= \begin{bmatrix} 0 & \lambda \\ \mu & k_s(y_2'-y_1') \end{bmatrix} \\
\mathbf{A}_{31}^{eff} &= \begin{bmatrix} 0 & \mu(1-y_2+y_1) \\ \lambda(1-y_2+y_1) & k_s(y_2'-y_1') \end{bmatrix} \\
\mathbf{A}_{33}^{eff} &= \begin{bmatrix} (1-y_2+y_1)\mu & 2k_s(y_2'-y_1') \\ k_s(y_2'-y_1') & (1-y_2+y_1)(\lambda+2\mu) \end{bmatrix}
\end{aligned} \tag{54}$$

$$\begin{aligned}
\mathbf{D}_1^{eff} &= \begin{bmatrix} 0 & 0 \\ 0 & -k_s(y_2''-y_1'') \end{bmatrix}, \\
\mathbf{D}_3^{eff} &= \begin{bmatrix} 0 & 0 \\ -k_s(y_2''-y_1'') & \dfrac{4\mu(\lambda+\mu)}{\lambda+2\mu}(y_2'-y_1') \end{bmatrix}
\end{aligned} \tag{55}$$

$$\nabla \cdot \boldsymbol{\sigma}^* = \begin{bmatrix} -2\tau^0(y_1''-y_2'') \\ 0 \end{bmatrix} \tag{56}$$

There are several observations that emerge from this homogenization process. First, the surface roughness seems to endow the body with finite elastic moduli even when those elastic moduli are zero in the original material which is rather unexpected. Specifically, C_{3331}^{eff}, C_{3133}^{eff}, C_{3313}^{eff}, and C_{1333}^{eff} are no longer null but are functions of the surface roughness as well as the surface elastic properties. Second, both the surface roughness and the surface elasticity disrupt the major and minor symmetries of the effective elasticity tensor. Specifically, since $C_{3133}^{eff} \neq C_{1333}^{eff}$ and $C_{1313}^{eff} \neq C_{3113}^{eff}$, it results in a non-symmetric stress tensor in the effective layer. This implies that the rough surface with elasticity endows the body with a body moment in the effective layer which breaks the symmetry of the stress tensor. Third, we observe that although the bulk material is homogeneous, some of the components of the effective elasticity tensor vary along the x_3 direction, since y_1 and y_2 are functions of x_3. This is a direct consequence of averaging between the two limits of the surface roughness profile. Finally, the residual stress of the surface τ^0 is manifested as a residual stress $\boldsymbol{\sigma}^*$ in the effective layer after homogenization. In Eq. $(53)_2$, the two terms on the right-hand side involve first derivatives of the macroscopic displacement but do not contribute to the divergence of the stress term. Taken together, they contribute to a force term in the equilibrium equation in the effective layer. This is in contrast to the equilibrium equation in the bulk material $(53)_1$ which does not involve a force term.

5 Numerical Calculations and Discussion

To gain insights into the implications of a highly rough surface on the mechanical response of materials, especially, nanostructures, we evaluate our results numerically for the case of uniaxial tensile deformation of a thin film, albeit with a very rough surface. We also examine by comparison the effect of high degree of roughness (based on the present work) versus gentle roughness (based on the work of Mohammadi et al. [46]). To this end, we start by considering a sinusoidal profile for the surface roughness.

5.1 Explicit Effective Properties for a Sinusoidal Roughness. First, we obtain explicit expressions for effective elastic properties for a rough surface with a sinusoidal roughness of the form,

$$f(x_1) = \frac{\delta}{2}\cos\left(2\pi\frac{x_1}{\varepsilon}\right) \tag{57}$$

Introducing the slow variable y,

$$f(y) = \frac{\delta}{2}\cos(2\pi y) \tag{58}$$

the two inverses of the function $f(y)$ in the [0,1] interval, for $x_3 =$ constant, are

$$y_1 = \frac{1}{2\pi}\arccos\left(2\frac{x_3}{\delta}\right) \quad \text{and} \quad y_2 = \frac{1}{2\pi}\arcsin\left(2\frac{x_3}{\delta}\right) + \frac{3}{4} \tag{59}$$

Using Eq. (59), the effective matrices $\mathbf{A}_{hk}^{eff}$, $\{h, k\} = \{1, 3\}$ become,

$$\begin{aligned}
\mathbf{A}_{11}^{eff} &= \begin{bmatrix} (\lambda+2\mu)p(x_3) & 0 \\ 0 & \mu\, p(x_3) \end{bmatrix}, \quad \mathbf{A}_{13}^{eff} = \begin{bmatrix} 0 & \lambda \\ \mu & \frac{k_s}{\delta}\, g(x_3) \end{bmatrix} \\
\mathbf{A}_{31}^{eff} &= \begin{bmatrix} 0 & \mu\, p(x_3) \\ \lambda\, p(x_3) & \frac{k_s}{\delta}\, g(x_3) \end{bmatrix}, \quad \mathbf{A}_{33}^{eff} = \begin{bmatrix} \mu\, p(x_3) & 2\frac{k_s}{\delta}\, g(x_3) \\ \frac{k_s}{\delta}\, g(x_3) & (\lambda+2\mu)\, p(x_3) \end{bmatrix}
\end{aligned} \tag{60}$$

where we have introduced the following for simplification,

$$p(x_3) = \frac{1}{\pi}\arccos\left(2\frac{x_3}{\delta}\right) \quad \text{and} \quad g(x_3) = \frac{2}{\pi\sqrt{1-\left(2\frac{x_3}{\delta}\right)^2}} \tag{61}$$

5.1 Extending these results to random roughness. The results for sinusoidal roughness can be extended to a general roughness by assuming that the roughness is statistically invariant over a length scale Λ. Then, without loss of generality, $f_0(x_1)$ can be considered to be a periodic function with a large enough period Λ where $f(x_1) = \delta f_0(x_1)$. Applying Fourier analysis, $f_0(x_1)$ can be expressed as a superposition of sinusoidal waves. Furthermore, for random roughness, we can consider an ensemble of general surfaces with specified autocorrelation function and correlation length, which are statistical properties of the random roughness. We then assume that for a random roughness, $f_0(x_1)$ is even and periodic with the period being larger than the correlation length. Expressing the profile for a general roughness as a Fourier series and applying the statistical properties for random surfaces should provide an avenue for extending the results for the sinusoidal roughness to the case of random roughness. However, such an analysis, although possible, is beyond the scope of this work. Moreover, we emphasize that such an analysis will necessarily have to be numerical and will be an interesting future study.

5.2 The Effective Young's Modulus of a Thin Film. We now consider a thin film of thickness h with a surface roughness profile given by Eq. (57). We apply our homogenization scheme and then study the response of the effective thin film under plane strain conditions subjected to uniaxial tensile deformation along the x_1 direction. Knowing that the traction along $\mathbf{e}_3$ is zero, gives the following two equations in the effective layer:

$$\begin{aligned}
\sigma_{13} &= 2\mu p(x_3)\varepsilon_{13} + \frac{k_s}{\delta}g(x_3)\varepsilon_{33} = 0 \\
\sigma_{33} &= \lambda p(x_3)\varepsilon_{11} + 2\frac{k_s}{\delta}g(x_3)\varepsilon_{13} + p(x_3)(\lambda+2\mu)\varepsilon_{33} = 0
\end{aligned} \tag{62}$$

Thus, ε_{13} and ε_{33} can be written in terms of ε_{11} as

$$\varepsilon_{33} = \frac{\lambda\mu p(x_3)^2}{J(x_3)}\varepsilon_{11} \quad \text{and} \quad \varepsilon_{13} = \frac{-\lambda\frac{k_s}{\delta}p(x_3)g(x_3)}{J(x_3)}\varepsilon_{11} \tag{63}$$

where we have defined

$$J(x_3) = \frac{2k_s^2}{\delta^2} g(x_3)^2 - \mu(\lambda + 2\mu) p(x_3)^2 \tag{64}$$

From equations (63), we get the remaining stress components in terms of ε_{11} as,

$$\sigma_{11} = \left[(\lambda + 2\mu) p(x_3) + \frac{\lambda^2 \mu p(x_3)^2}{J(x_3)} \right] \varepsilon_{11} \quad \text{and}$$
$$\sigma_{31} = -\frac{\lambda\mu \frac{k_s}{\delta} g(x_3) p(x_3)}{J(x_3)} \varepsilon_{11} \tag{65}$$

Therefore, the strain energy density of the effective layer (region B_2 in Fig. 1(*b*)) is

$$W_{\text{layer}} = \frac{1}{2} A \varepsilon_{11}^2 \int_{-(\delta/2)}^{\delta/2} \left[(\lambda + \mu) p(x_3) + \frac{\lambda^2 \mu p(x_3)^2}{J(x_3)} + \frac{\lambda^2 \mu \frac{k_s^2}{\delta^2} g(x_3)^2 p(x_3)^2}{J(x_3)^2} \right] dx_3 \tag{66}$$

Using Taylor series expansion of the integrand, we obtain

$$W_{\text{layer}} = \frac{1}{2} A \varepsilon_{11}^2 \left[\frac{\delta\lambda}{2} + \delta\mu - \frac{16\pi^4 (12 + \pi^2) \delta^7 \lambda^2 \mu^3 (\lambda + 2\mu)^2 k_s^2}{3(\pi^2 \delta^2 \mu(\lambda + 2\mu) - 32k_s^2)^4} + \frac{2048\pi^2 (12 + \pi^2) \delta^5 \lambda^2 \mu^2 (\lambda + 2\mu) k_s^4}{3(\pi^2 \delta^2 \mu(\lambda + 2\mu) - 32k_s^2)^4} - \frac{\pi^2 \delta^3 \lambda^2 \mu}{\pi^2 \delta^2 \mu(\lambda + 2\mu) - 32k_s^2} + \frac{16\pi^2 \delta^3 \lambda^2 \mu k_s^2}{(\pi^2 \delta^2 \mu(\lambda + 2\mu) - 32k_s^2)^2} - \frac{16384(\pi^2 - 4) \delta^3 \lambda^2 \mu k_s^6}{(\pi^2 \delta^2 \mu(\lambda + 2\mu) - 32k_s^2)^4} \right] \tag{67}$$

The strain energy density in the bulk (region B_1 in Fig. 1(*b*)) with thickness $h - \delta$ is obtained as,

$$W_{\text{bulk}} = \frac{1}{2} A (h - \delta) \frac{4\mu(\lambda + \mu)}{\lambda + 2\mu} \varepsilon_{11}^2 \tag{68}$$

Denoting the total strain energy density as W^1_{total} and the effective Young's modulus as E_1^{eff}, we have,

$$\frac{\partial^2 W^1_{\text{total}}}{\partial \varepsilon_{11}^2} = \frac{\partial^2 (W_{\text{bulk}} + W_{\text{layer}})}{\partial \varepsilon_{11}^2} = A h E_1^{eff} \tag{69}$$

Thus, for a thin film with a rough surface, multiscale homogenization yields the following effective Young's modulus,

$$\begin{aligned} E_1^{eff} = {} & \left(1 - \frac{\delta}{h}\right) \frac{4\mu(\lambda + \mu)}{\lambda + 2\mu} + \frac{\delta}{h} \left(\frac{1}{6\left(\pi^2 \delta^2 \mu(\lambda + 2\mu) - 32k_s^2\right)^4} \right) \\ & \times \left[-32\pi^4 \left(12 + \pi^2\right) \delta^6 \lambda^2 \mu^3 (\lambda + 2\mu)^2 k_s^2 \right. \\ & + 4096\pi^2 \left(12 + \pi^2\right) \delta^4 \lambda^2 \mu^2 (\lambda + 2\mu) k_s^4 \\ & - 98304\left(\pi^2 - 4\right) \delta^2 \lambda^2 \mu k_s^6 - 6\pi^2 \delta^2 \lambda^2 \mu \left(\pi^2 \delta^2 \mu(\lambda + 2\mu) - 32k_s^2\right)^3 \\ & + 96\pi^2 \delta^2 \lambda^2 \mu k_s^2 \left(\pi^2 \delta^2 \mu(\lambda + 2\mu) - 32k_s^2\right)^2 \\ & + 3\lambda \left(\pi^2 \delta^2 \mu(\lambda + 2\mu) - 32k_s^2\right)^4 \\ & \left. + 6\mu \left(\pi^2 \delta^2 \mu(\lambda + 2\mu) - 32k_s^2\right)^4 \right] \end{aligned} \tag{70}$$

We compare this expression with the results of Mohammadi et al. [46] for a thin film with sinusoidal roughness under uniaxial tension. If the effective surface elastic constant obtained by them has the following expression,

$$k_s^{eff} = k_s - \frac{2\pi}{\varepsilon} \delta^2 \frac{4\mu(\lambda + \mu)}{\lambda + 2\mu} \tag{71}$$

the strain energy for a thin film of thickness h with a homgenized flat surface characterized by k_s^{eff} is given as

$$W^2_{\text{total}} = \frac{1}{2} A k_s^{eff} \varepsilon_{11}^2 + A\tau^0 \varepsilon + \frac{1}{2} A h \frac{4\mu(\lambda + \mu)}{\lambda + 2\mu} \varepsilon_{11}^2 \tag{72}$$

where the first two terms arise from the homogenized surface and the last term is the contribution from the bulk. Then, the effective Young's modulus is obtained as

$$E_2^{eff} = \frac{k_s}{h} + \frac{4\mu(\lambda + \mu)}{\lambda + 2\mu} \left[1 - \frac{2\pi}{\varepsilon h} \delta^2 \right] \tag{73}$$

We wish to emphasize that the effective Young's modulus derived from the work of Ref. [46] (Eq. (73)) depends on the wavelength whereas in our work (Eq. (70)) it does not. While the wavelength is a characteristic of the surface profile, the separation of scales in multiscale homogenization is enforced by assuming ε to be very small compared to the amplitude δ or rather $\delta/\varepsilon \gg 1$. Although ε does not enter explicitly in our final results, we will work within the limit that $\varepsilon/\delta \ll 1$ which corresponds to a very rough surface. In that sense, our work and that of Mohammadi et al. [46] present two extreme cases for surfaces with varying degree of roughness.

We now examine E_1^{eff} and E_2^{eff} numerically to gain more insights. We consider a thin film of Cu with $\lambda = 91$ GPa and $\mu = 43$ GPa, and $k_s = \lambda_s + 2\mu_s = -3.16$ N/m. We use these material constants for a (001) Cu surface taken from Ref. [55] and take the wavelength, ε, to be 10 nm to facilitate comparison with numerical calculations of Ref. [46]. We note that our theoretical model is applicable for any wavelength as long as the high roughness approximation is satisfied. Furthermore, although the present numerical example uses material parameters derived from atomistic simulations using embedded-atom method (EAM) potentials [55], our model can be used with material parameters obtained from experiments or computed from more sophisticated methods such as density functional theory (DFT) for more accurate predictions of surface properties. Since this work is focused on very rough surfaces with large amplitude while in Ref. [46], the roughness amplitude is smaller than the wavelength, we plot the E^{eff} normalized with respect to $E_{Cu} = 4\mu(\lambda + \mu)/(\lambda + 2\mu)$ as a function of the film thickness h ranging from δ to 10δ.

Figures 3(*a*) and 3(*b*) reveal that while in both cases the film has a softer elastic behavior as the amplitude of the roughness becomes comparable to the film thickness, a highly rough surface has a more dramatic impact on the effective Young's modulus than a surface with mild roughness. Specifically, the Young's modulus of the film is reduced to 30% for high roughness while it only reduces to 70% for mild or gentle roughness. When the film thickness becomes much larger than the roughness amplitude, the rough surface has a negligible effect on the Young's modulus.

In order to understand the contribution of surface energy and surface roughness on the effective properties of the homogenized

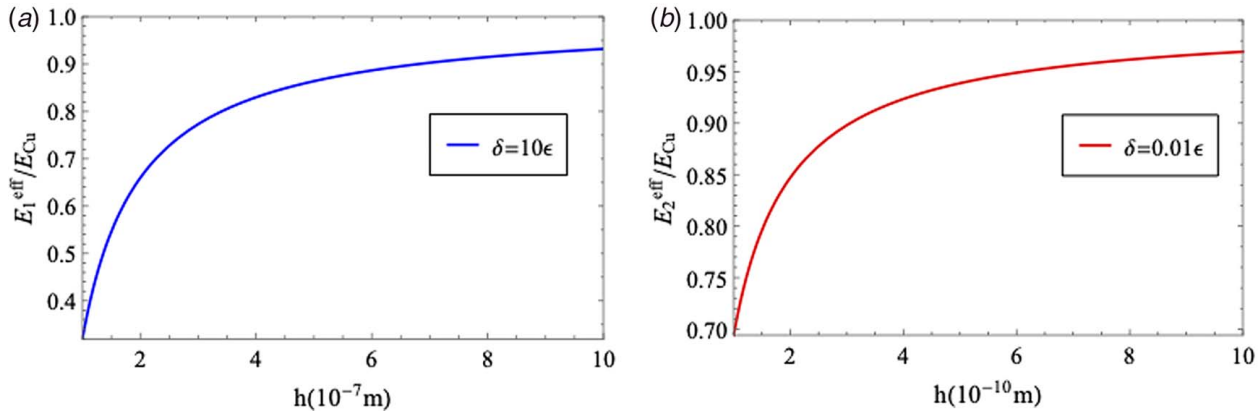

Fig. 3 (*a*) E_1^{eff}/E_{Cu} as a function of film thickness for $\delta = 10\epsilon$ (high roughness). (*b*) E_2^{eff}/E_{Cu} as a function of film thickness for $\delta = 0.01\epsilon$ (mild roughness). $\varepsilon = 10$ nm. h varies from δ to 10δ. Here, δ is the amplitude and ε is the wavelength of the roughness. E_1^{eff} and E_1^{eff} are the effective Young's modulus of a thin film with a rough surface using our method and the method of Mohammadi et al. [46] respectively while E_{Cu} is the Young's modulus of Cu.

thin film, we compare the effective Young's modulus of the thin film with and without surface energy effects. To this end, we first derive explicitly the homogenization results of Nevard and Keller [47] for a very rough surface and use them to obtain an expression for the Young's modulus of a thin film with sinusoidal roughness (Appendix B).

Figures 4(*a*) and 4(*b*) show the results for our model and the model by Mohammadi et al. [46] for roughness with small amplitude ($\delta = 0.01\varepsilon$) whereas Figs. 4(*c*) and 4(*d*) compare their results for roughness with large amplitude ($\delta = 10\varepsilon$). As seen in Fig. 4(*b*), the model in [46] predicts that a gentle rough surface without surface elasticity does not change the Young's modulus considerably. This is expected since it is very close to a flat surface. However, including surface energy effects even with gentle roughness results in a noticeable softening. Comparing this to Fig. 4(*a*), we note that our approach predicts a significant reduction in the Young's modulus even when the roughness is very small. An even more curious outcome is that including surface elasticity

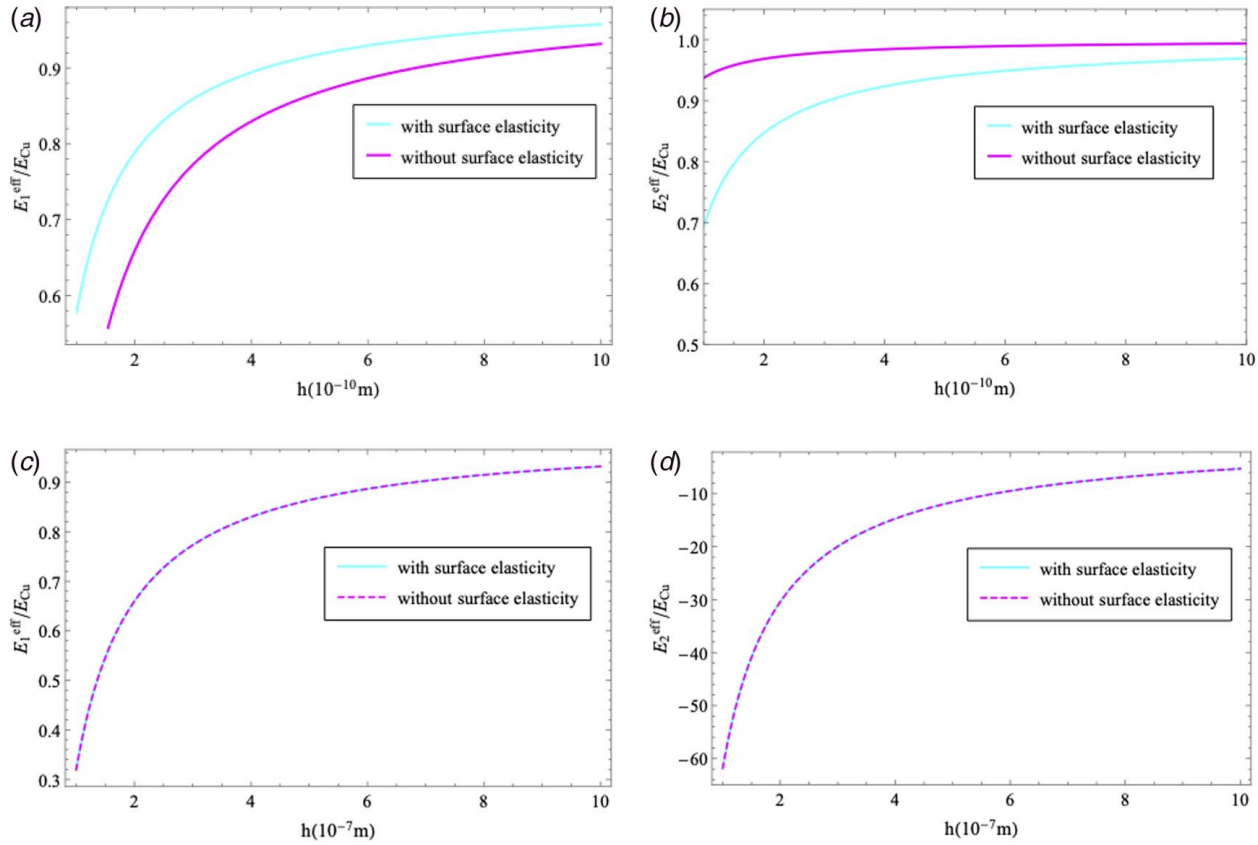

Fig. 4 (*a*) E_1^{eff}/E_{Cu} with and without surface effects as a function of the film thickness for gentle roughness ($\delta = 0.01\varepsilon$). (*b*) E_2^{eff}/E_{Cu} with and without surface effects as a function of the film thickness for gentle roughness ($\delta = 0.01\varepsilon$). (*c*) E_1^{eff}/E_{Cu} with and without surface effects as a function of the film thickness for high roughness ($\delta = 10\varepsilon$). (*d*) E_2^{eff}/E_{Cu} with and without surface effects as a function of the film thickness for high roughness ($\delta = 10\varepsilon$). Film thickness h varies from δ to 10δ and $\varepsilon = 10$ nm. Here, δ is the amplitude and ε is the wavelength of the roughness. E_1^{eff} and E_1^{eff} are the effective Young's modulus of a thin film with a rough surface using our method and the method of [46] respectively while E_{Cu} is the Young's modulus of Cu.

results in a slight increase in the Young's modulus. This is physically unreasonable since the numerical calculations based on Ref. [46] study shows that surface effects should cause softening for Cu. This implies that since the multi-scale homogenization treats the roughness as an equivalent layer of finite thickness, it may not be suitable for modeling rough surfaces with very small amplitudes. In the case of very rough surfaces, Fig. 4(*c*) based on our homogenization method reveals that roughness has a dominant effect, and hence, curves with and without surface energy effects are identical. Figure 4(*d*) shows that the model by Ref. [46] gives physically unreasonable results for the case of very rough surfaces. Taken together, Fig. 4 provides clear evidence that the multi-scale homogenization and conventional homogenization based on perturbation method yield two limiting cases for rough surfaces with large amplitudes and rough surfaces with very small amplitudes respectively. We wish to note that we do not know the range of validity of either of these approaches for intermediate values of surface roughness and hence a direct quantitative comparison of our results obtained for high roughness with those presented for weak roughness in prior studies [44,46] is not possible. A theoretical analysis of the limits of validity of our method for intermediate surface roughness is beyond the scope of the present study.

5.3 Curvature-dependent Surface Energy. Here, we demonstrate that the multi-scale homogenization approach furnishes a way to establish a connection with the Steigmann-Ogden theory for curvature-dependent surface elasticity [40]. The homogenized system obtained by way of multi-scale homogenization method replaces the surface with a roughness of amplitude δ with an equivalent layer of thickness δ with effective bulk properties. This endows the equivalent layer with a bending stiffness even if we do not consider curvature-dependent surface energy in our original model. As shown by Chhapadia et al. [43], the Steigmann-Ogden surface energy constants can be used to define the thickness of a surface t as a ratio of the energy contribution due to bending and stretching, and is given by

$$t = \sqrt{\frac{C_1}{C_0}} \tag{74}$$

where C_0 and C_1 are surface elastic modulus and Steigmann-Ogden constant, respectively. Interestingly, our method naturally yields that the thickness of the rough surface is the amplitude δ. Furthermore, according to [43], based on the Gurtin-Murdoch theory, the renormalized effective elastic modulus in tension can be written in the following form:

$$\frac{E^{eff}}{E} = 1 + \frac{4C_0}{hE} \tag{75}$$

In order to compare our results with (75), we can write (70) as a function of film thickness h by substituting the elastic moduli for Cu mentioned earlier, and specifying a value for δ. The equation has the form:

$$\frac{E^{eff}}{E}(h) = 1 - \frac{\alpha}{h} \tag{76}$$

where α is some numerical constant. Comparing (75) and (B26), we can obtain an estimate for C_0. Then, substituting δ for the thickness of the surface in (74), we can provide a rough estimate for C_1.

For numerical calculations, we use two values of δ – 1 nm and 10 nm – to compute the estimates for C_0 and C_0 for rough surfaces with small amplitude and large amplitude. For $\delta = 1$ nm, we get $C_0 = -9.0571$ J/m^2 ($= -0.5653$ eV/Å^2) and $C_1 = -1.963 \times 10^{-17}$ J ($= -122.528$ eV). The values are comparable to those obtained by Chhapadia et al. [43]. For $\delta = 10$ nm, we get $C_0 = -221.261$ J/m^2 ($= -13.81$ eV/Å^2) and $C_1 = -2.2169 \times 10^{-14}$ J ($= -138369.27$ eV). The large value for C_1 for large amplitude is expected since a layer of larger thickness would have greater bending stiffness. However, we do emphasize that these are rough estimates simply to demonstrate that multi-scale homogenization provides a simple way to determine curvature-dependent surface energy constants. For more accurate estimates, one would need to equate the homogenized thin film to an equivalent thin film with a flat surface including curvature-dependent surface energy and would be an interesting future study.

6 Conclusion

In this work, we have extended the multi-scale homogenization method of Nevard and Keller [47] for highly rough surfaces to take into account the effect of surface energy. The novelty of the method is that it replaces the highly rough surface by a layer of finite thickness with effective bulk elastic properties as opposed to a flat surface with effective surface properties furnished by conventional perturbation methods. We obtain analytical expressions for a general highly rough surface and specialize our results for the case of a thin film with a sinusoidal roughness. Using numerical calculations, we compare our results with those based on the work of Mohammadi et al. [46] which treats the rough surface as a perturbation about a flat surface. Our study shows that the two methods provide two limiting cases for surface roughness. Specifically, homogenization based on perturbation methods are appropriate for gentle roughness with small amplitude but high roughness with large amplitude necessitates the use of multi-scale homogenization. We also show that the multi-scale homogenization approach furnishes a natural way for estimating curvature-dependent surface energy constants based on the Steigmann–Ogden theory [40].

Acknowledgment

We gratefully acknowledge the support of NSF under grant DMR-1508484. We also acknowledge the use of the Maxwell cluster and the support from the Research Computing Data Core at the University of Houston. We thank Professor Pradeep Sharma and Dr. Sana Krichen for insightful discussions.

Conflict of Interest

There are no conflicts of interest.

Data Availability Statement

The authors attest that all data for this study are included in the paper. Data provided by a third party listed in Acknowledgment.

Appendix A: Introduction of Separation of Scales

Using the relation between $\mathbf{u}(x_1, x_3)$ and $\mathbf{U}(x_1, x_3, y)$ (Eqs. (16) and (17)), the equilibrium equation (18) becomes,

$$\mathbf{A}_{11}(\mathbf{U}_{,11} + \varepsilon^{-1}\mathbf{U}_{,1y} + \varepsilon^{-1}\mathbf{U}_{,y1} + \varepsilon^{-2}\mathbf{U}_{,yy}) + \mathbf{A}_{13}(\mathbf{U}_{,31} + \varepsilon^{-1}\mathbf{U}_{,3y}) + \mathbf{A}_{31}(\mathbf{U}_{,13} + \varepsilon^{-1}\mathbf{U}_{,y3}) + \mathbf{A}_{33}\mathbf{U}_{,33} = 0, \quad x_3 < h(y) \tag{A1}$$

The left-hand side and right-hand side of the boundary condition are obtained, respectively, as

$$(\mathbf{A}_{hk}\mathbf{u}_{,k})\mathbf{n}_h = -\varepsilon^{-2}(h_y\mathbf{A}_{11}\mathbf{U}_{,y}) + \varepsilon^{-1}(-h_y\mathbf{A}_{11}\mathbf{U}_{,1} - h_y\mathbf{A}_{13}\mathbf{U}_{,3} + \mathbf{A}_{31}\mathbf{U}_{,y}) + \mathbf{A}_{31}\mathbf{U}_{,1} + \mathbf{A}_{33}\mathbf{U}_{,3} \tag{A2}$$

$$\begin{aligned}
\|\mathbf{n}\|\mathrm{div}_s\mathbf{S}_s = \varepsilon^2 &\left[\frac{\mathbf{B}_{11}^{(4)}}{h_y^4}\mathbf{U}_{,yy} + \frac{\mathbf{B}_{11}^{(3)}}{h_y^3}(\mathbf{U}_{,1y} + \mathbf{U}_{,y1}) + \frac{\mathbf{B}_{11}^{(2)}}{h_y^2}\mathbf{U}_{,11} + \frac{\mathbf{B}_{13}^{(2)}}{h_y^2}\mathbf{U}_{,13} + \frac{\mathbf{B}_{31}^{(2)}}{h_y^2}\mathbf{U}_{,31} + \frac{\mathbf{B}_{13}^{(3)}}{h_y^3}\mathbf{U}_{,y3} + \frac{\mathbf{B}_{31}^{(3)}}{h_y^3}\mathbf{U}_{,3y} + \frac{\mathbf{B}_{33}^{(2)}}{h_y^2}\mathbf{U}_{,33}\right.\\
&\left. + \frac{h_{yy}}{h_y^4}\mathbf{D}_1^{(2)}\mathbf{U}_{,1} + \frac{h_{yy}}{h_y^5}\mathbf{D}_1^{(3)}\mathbf{U}_{,y} + \frac{h_{yy}}{h_y^4}\mathbf{D}_3^{(2)}\mathbf{U}_{,3} + \frac{h_{yy}}{h_y^4}\mathbf{T}^{(2)}\right] + \varepsilon\left[\frac{\mathbf{B}_{11}^{(3)}}{h_y^3}\mathbf{U}_{,yy} + \frac{\mathbf{B}_{11}^{(2)}}{h_y^2}(\mathbf{U}_{,1y} + \mathbf{U}_{,y1}) + \frac{\mathbf{B}_{11}^{(1)}}{h_y}\mathbf{U}_{,11} + \frac{\mathbf{B}_{13}^{(1)}}{h_y}\mathbf{U}_{,13}\right.\\
&\left. + \frac{\mathbf{B}_{13}^{(2)}}{h_y^2}\mathbf{U}_{,y3} + \frac{\mathbf{B}_{31}^{(1)}}{h_y}\mathbf{U}_{,31} + \frac{\mathbf{B}_{31}^{(2)}}{h_y^2}\mathbf{U}_{,3y} + \frac{\mathbf{B}_{33}^{(1)}}{h_y}\mathbf{U}_{,33} + \frac{h_{yy}}{h_y^3}\mathbf{D}_1^{(1)}\mathbf{U}_{,1} + \frac{h_{yy}}{h_y^4}\mathbf{D}_1^{(2)}\mathbf{U}_{,y} + \frac{h_{yy}}{h_y^3}\mathbf{D}_3^{(1)}\mathbf{U}_{,3} + \frac{h_{yy}}{h_y^3}\mathbf{T}^{(1)}\right]\\
&+ \varepsilon^0\left[\frac{\mathbf{B}_{11}^{(2)}}{h_y^2}\mathbf{U}_{,yy} + \frac{\mathbf{B}_{11}^{(1)}}{h_y}(\mathbf{U}_{,y1} + \mathbf{U}_{,1y}) + \mathbf{B}_{13}^{(0)}\mathbf{U}_{,13} + \frac{\mathbf{B}_{13}^{(1)}}{h_y}\mathbf{U}_{,y3} + \mathbf{B}_{31}^{(0)}\mathbf{U}_{,31} + \frac{\mathbf{B}_{31}^{(1)}}{h_y}\mathbf{U}_{,3y} + \mathbf{B}_{33}^{(0)}\mathbf{U}_{,33}\right.\\
&\left. + \frac{h_{yy}}{h_y^3}\mathbf{D}_1^{(1)}\mathbf{U}_{,y} + \frac{h_{yy}}{h_y^2}\mathbf{D}_1^{(0)}\mathbf{U}_{,1} + \frac{h_{yy}}{h_y^2}\mathbf{D}_3^{(0)}\mathbf{U}_{,3} + \frac{h_{yy}}{h_y^2}\mathbf{T}^{(0)}\right] + \varepsilon^{-1}\left[\frac{\mathbf{B}_{11}^{(1)}}{h_y}\mathbf{U}_{,yy} + \mathbf{B}_{13}^{(0)}\mathbf{U}_{,y3} + \mathbf{B}_{31}^{(0)}\mathbf{U}_{,3y} + h_y\mathbf{B}_{33}^{(-1)}\mathbf{U}_{,33} + \frac{h_{yy}}{h_y^2}\mathbf{D}_1^{(0)}\mathbf{U}_{,y}\right.\\
&\left. + \varepsilon^{-1}\frac{h_{yy}}{h_y}\mathbf{D}_3^{(-1)}\mathbf{U}_{,y} + \frac{h_{yy}}{h_y}\mathbf{T}^{(-1)}\right] + o(\varepsilon^2)
\end{aligned} \tag{A3}$$

where $h_y = dh/dy$ and $h_{yy} = d^2h/dy^2$. The $\mathbf{B}$ matrices have the following expressions:

$$\begin{aligned}
\mathbf{B}_{11} &= \begin{bmatrix} -\frac{\epsilon^3}{h_y^3}(\lambda_s + 2\mu_s) & -\frac{\epsilon^4}{h_y^4}\left(\frac{3}{2}\lambda_s + 2\mu_s\right) + \frac{\epsilon^2}{h_y^2}(\lambda_s + 2\mu_s) \\ -\frac{\epsilon^4}{h_y^4}\left(\frac{3}{2}\lambda_s + \mu_s\right) + \frac{\epsilon^2}{h_y^2}(\lambda_s + 2\mu_s) & -\frac{\epsilon^3}{h_y^3}\left(\frac{3}{2}\lambda_s + 2\mu_s\right) + \frac{\varepsilon}{h_y}(\lambda_s + 2\mu_s) \end{bmatrix}\\
&= \frac{\varepsilon^4}{h_y^4}\mathbf{B}_{11}^{(4)} + \frac{\varepsilon^3}{h_y^3}\mathbf{B}_{11}^{(3)} + \frac{\varepsilon^2}{h_y^2}\mathbf{B}_{11}^{(2)} + \frac{\varepsilon}{h_y}\mathbf{B}_{11}^{(1)}
\end{aligned} \tag{A4}$$

$$\begin{aligned}
\mathbf{B}_{13} &= \begin{bmatrix} (\lambda_s + 2\mu_s)\frac{\varepsilon^2}{h_y^2} & -\frac{3}{2}(2\mu_s + \lambda_s)\frac{\varepsilon^3}{h_y^3} + (2\mu_s + \lambda_s)\frac{\varepsilon}{h_y} \\ -\frac{3}{2}(2\mu_s + \lambda_s)\frac{\varepsilon^3}{h_y^3} + (2\mu_s + \lambda_s)\frac{\varepsilon}{h_y} & -\frac{3}{2}(2\mu_s + \lambda_s)\frac{\varepsilon^2}{h_y^2} + (2\mu_s + \lambda_s) \end{bmatrix}\\
&= \mathbf{B}_{13}^{(0)} + \frac{\varepsilon}{h_y}\mathbf{B}_{13}^{(1)} + \frac{\varepsilon^2}{h_y^2}\mathbf{B}_{13}^{(2)} + \frac{\varepsilon^3}{h_y^3}\mathbf{B}_{13}^{(3)}
\end{aligned} \tag{A5}$$

$$\begin{aligned}
\mathbf{B}_{31} &= \begin{bmatrix} (\lambda_s + 2\mu_s)\frac{\varepsilon^2}{h_y^2} & -\frac{3}{2}(2\mu_s + \lambda_s)\frac{\varepsilon^3}{h_y^3} + (2\mu_s + \lambda_s)\frac{\varepsilon}{h_y} \\ -\left(\frac{3}{2}\lambda_s + 2\mu_s\right)\frac{\varepsilon^3}{h_y^3} + (2\mu_s + \lambda_s)\frac{\varepsilon}{h_y} & -\frac{3}{2}(2\mu_s + \lambda_s)\frac{\varepsilon^2}{h_y^2} + (2\mu_s + \lambda_s) \end{bmatrix}\\
&= \mathbf{B}_{31}^{(0)} + \frac{\varepsilon}{h_y}\mathbf{B}_{31}^{(1)} + \frac{\varepsilon^2}{h_y^2}\mathbf{B}_{31}^{(2)} + \frac{\varepsilon^3}{h_y^3}\mathbf{B}_{31}^{(3)}
\end{aligned} \tag{A6}$$

$$\begin{aligned}
\mathbf{B}_{33} &= \begin{bmatrix} (\lambda_s + 2\mu_s)\frac{\varepsilon}{h_y} & -\frac{3}{2}(2\mu_s + \lambda_s)\frac{\varepsilon^2}{h_y^2} + (2\mu_s + \lambda_s) \\ -\frac{3}{2}(2\mu_s + \lambda_s)\frac{\varepsilon^2}{h_y^2} + (2\mu_s + \lambda_s) & -\frac{3}{2}(2\mu_s + \lambda_s)\frac{\varepsilon}{h_y} + \varepsilon^{-1}h_y(2\mu_s + \lambda_s) \end{bmatrix}\\
&= \varepsilon^{-1}h_y\mathbf{B}_{33}^{(-1)*} + \mathbf{B}_{33}^{(0)} + \frac{\varepsilon}{h_y}\mathbf{B}_{33}^{(1)} + \frac{\varepsilon^2}{h_y^2}\mathbf{B}_{33}^{(2)}
\end{aligned} \tag{A7}$$

where

$$\begin{aligned}
\mathbf{B}_{11}^{(1)} &= \begin{bmatrix} 0 & 0 \\ 0 & \lambda_s + 2\mu_s \end{bmatrix}, \quad \mathbf{B}_{11}^{(2)} = \begin{bmatrix} 0 & \lambda_s + 2\mu_s \\ \lambda_s + 2\mu_s & 0 \end{bmatrix}\\
\mathbf{B}_{11}^{(3)} &= \begin{bmatrix} -(\lambda_s + 2\mu_s) & 0 \\ 0 & -\left(\frac{3}{2}\lambda_s + 2\mu_s\right) \end{bmatrix}, \quad \mathbf{B}_{11}^{(4)} = \begin{bmatrix} 0 & 0 \\ 0 & \lambda_s + 2\mu_s \end{bmatrix}
\end{aligned} \tag{A8}$$

$$\mathbf{B}_{13}^{(0)}=\begin{bmatrix}0 & 0\\ 0 & \lambda_s+2\mu_s\end{bmatrix},\ \mathbf{B}_{13}^{(1)}=\begin{bmatrix}0 & \lambda_s+2\mu_s\\ \lambda_s+2\mu_s & 0\end{bmatrix}$$
$$\mathbf{B}_{13}^{(2)}=\begin{bmatrix}-(\lambda_s+2\mu_s) & 0\\ 0 & -\frac{3}{2}(\lambda_s+2\mu_s)\end{bmatrix},\ \mathbf{B}_{13}^{(3)}=\begin{bmatrix}0 & -\frac{3}{2}(\lambda_s+2\mu_s)\\ -\frac{3}{2}(\lambda_s+2\mu_s) & \end{bmatrix} \tag{A9}$$

$$\mathbf{B}_{31}^{(0)}=\begin{bmatrix}0 & 0\\ 0 & \lambda_s+2\mu_s\end{bmatrix},\ \mathbf{B}_{31}^{(1)}=\begin{bmatrix}0 & \lambda_s+2\mu_s\\ \lambda_s+2\mu_s & 0\end{bmatrix}$$
$$\mathbf{B}_{31}^{(2)}=\begin{bmatrix}-(\lambda_s+2\mu_s) & 0\\ 0 & -\frac{3}{2}(\lambda_s+2\mu_s)\end{bmatrix},\ \mathbf{B}_{31}^{(3)}=\begin{bmatrix}0 & -\left(\frac{3}{2}\lambda_s+2\mu_s\right)\\ -\left(\frac{3}{2}\lambda_s+2\mu_s\right) & \end{bmatrix} \tag{A10}$$

$$\mathbf{B}_{33}^{(-1)}=\begin{bmatrix}0 & 0\\ 0 & \lambda_s+2\mu_s\end{bmatrix},\ \mathbf{B}_{33}^{(0)}=\begin{bmatrix}0 & \lambda_s+2\mu_s\\ \lambda_s+2\mu_s & 0\end{bmatrix}$$
$$\mathbf{B}_{33}^{(1)}=\begin{bmatrix}\lambda_s+2\mu_s & 0\\ 0 & -\frac{3}{2}(\lambda_s+2\mu_s)\end{bmatrix},\ \mathbf{B}_{33}^{(2)}=\begin{bmatrix}0 & -\frac{3}{2}(\lambda_s+2\mu_s)\\ -\frac{3}{2}(\lambda_s+2\mu_s) & 0\end{bmatrix} \tag{A11}$$

The **D** matrices have the following expressions:

$$\mathbf{D}_1=\begin{bmatrix}-\varepsilon^2\frac{h_{yy}}{h_y^4}(\lambda_s+2\mu_s) & \varepsilon^3\frac{h_{yy}}{h_y^5}(6\lambda_s+8\mu_s)-2\varepsilon\frac{h_{yy}}{h_y^3}(\lambda_s+2\mu_s)\\ \varepsilon^3\frac{h_{yy}}{h_y^5}\left(\frac{15}{2}\lambda_s+5\mu_s\right)-3\varepsilon\frac{h_{yy}}{h_y^3}(\lambda_s+2\mu_s) & \varepsilon^2\frac{h_{yy}}{h_y^4}(6\lambda_s+8\mu_s)-2\frac{h_{yy}}{h_y^2}(\lambda_s+2\mu_s)\end{bmatrix}$$
$$=\varepsilon^3\frac{h_{yy}}{h_y^5}\mathbf{D}_1^{(3)}+\varepsilon^2\frac{h_{yy}}{h_y^4}\mathbf{D}_1^{(2)}+\varepsilon\frac{h_{yy}}{h_y^3}\mathbf{D}_1^{(1)}+\frac{h_{yy}}{h_y^2}\mathbf{D}_1^{(0)} \tag{A12}$$

$$\mathbf{D}_3=\begin{bmatrix}-2\varepsilon\frac{h_{yy}}{h_y^3}(\lambda_s+2\mu_s) & -\frac{9}{2}\varepsilon^2\frac{h_{yy}}{h_y^4}(\lambda_s+2\mu_s)-(\lambda_s+2\mu_s)\frac{h_{yy}}{h_y^2}\\ \varepsilon^2\frac{h_{yy}}{h_y^4}(6\lambda_s+8\mu_s)-2(\lambda_s+2\mu_s)\frac{h_{yy}}{h_y^2} & -\frac{9}{2}\varepsilon\frac{h_{yy}}{h_y^3}(\lambda_s+2\mu_s)-\varepsilon^{-1}(\lambda_s+2\mu_s)\frac{h_{yy}}{h_y}\end{bmatrix}$$
$$=\varepsilon^2\frac{h_{yy}}{h_y^4}\mathbf{D}_3^{(2)}+\varepsilon\frac{h_{yy}}{h_y^3}\mathbf{D}_3^{(1)}+\frac{h_{yy}}{h_y^2}\mathbf{D}_3^{(0)}+\varepsilon^{-1}\frac{h_{yy}}{h_y}\mathbf{D}_3^{(-1)*} \tag{A13}$$

where

$$\mathbf{D}_1^{(0)}=\begin{bmatrix}0 & 0\\ 0 & -2(\lambda_s+2\mu_s)\end{bmatrix},\ \mathbf{D}_1^{(1)}=\begin{bmatrix}0 & -2(\lambda_s+2\mu_s)\\ -3(\lambda_s+2\mu_s) & 0\end{bmatrix}$$
$$\mathbf{D}_1^{(2)}=\begin{bmatrix}-3(\lambda_s+2\mu_s) & 0\\ 0 & (6\lambda_s+8\mu_s)\end{bmatrix},\ \mathbf{D}_1^{(3)}=\begin{bmatrix}0 & (6\lambda_s+8\mu_s)\\ \frac{15}{2}\lambda_s+5\mu_s & 0\end{bmatrix} \tag{A14}$$

$$\mathbf{D}_3^{(-1)}=\begin{bmatrix}0 & 0\\ 0 & -(\lambda_s+2\mu_s)\end{bmatrix},\ \mathbf{D}_3^{(0)}=\begin{bmatrix}0 & -(\lambda_s+2\mu_s)\\ -2(\lambda_s+2\mu_s) & 0\end{bmatrix}$$
$$\mathbf{D}_3^{(1)}=\begin{bmatrix}-2(\lambda_s+2\mu_s) & 0\\ 0 & \frac{9}{2}((\lambda_s+2\mu_s))\end{bmatrix},\ \mathbf{D}_3^{(2)}=\begin{bmatrix}0 & \frac{9}{2}(\lambda_s+2\mu_s)\\ 6\lambda_s+8\mu_s & 0\end{bmatrix} \tag{A15}$$

The **T** vector has the following expression:

$$\mathbf{T}=\begin{bmatrix}\frac{3}{2}\varepsilon^2\frac{h_{yy}}{h_y^4}\tau^0-\frac{h_{yy}}{h_y^2}\tau^0\\ \frac{3}{2}\varepsilon\frac{h_{yy}}{h_y^3}\tau^0-\varepsilon^{-1}\frac{h_{yy}}{h_y}\tau^0\end{bmatrix}=\varepsilon^2\frac{h_{yy}}{h_y^4}\mathbf{T}^{(2)}+\varepsilon\frac{h_{yy}}{h_y^3}\mathbf{T}^{(1)}+\frac{h_{yy}}{h_y^2}\mathbf{T}^{(0)}+\varepsilon^{-1}\frac{h_{yy}}{h_y}\mathbf{T}^{(-1)*} \tag{A16}$$

where

$$\mathbf{T}^{(-1)}=\begin{bmatrix}0\\ -\tau^0\end{bmatrix},\ \mathbf{T}^{(0)}=\begin{bmatrix}-\tau^0\\ 0\end{bmatrix},\ \mathbf{T}^{(1)}=\begin{bmatrix}0\\ \frac{3}{2}\tau^0\end{bmatrix},\ \mathbf{T}^{(2)}=\begin{bmatrix}\frac{3}{2}\tau^0\\ 0\end{bmatrix} \tag{A17}$$

Note that the superscript (−1) is used only for notation purposes to differentiate between the orders of ε *associated with different matrices and doesn't refer to the inverse of the matrix.*

Appendix B: Homogenized System in the Absence of Surface Elasticity

The boundary value problems for order ε^{-1} and ε^{0} in the absence of surface elasticity:
Order ε^{-1}:

$$\begin{cases} [\mathbf{A}_{11}\mathbf{u}^{(1)}_{,y} + \mathbf{A}_{11}\mathbf{u}^{(0)}_{,1} + \mathbf{A}_{13}\mathbf{u}^{(0)}_{,3}]_{,y} = 0, & x_3 < h(y) \\ h_y(-\mathbf{A}_{11}\mathbf{u}^{(1)}_{,y} - \mathbf{A}_{11}\mathbf{u}^{(0)}_{,1} - \mathbf{A}_{13}\mathbf{u}^{(0)}_{,3}) = 0, & x_3 = h(y) \end{cases} \tag{B1}$$

Order ε^{0}:

$$\begin{cases} [\mathbf{A}_{11}\mathbf{u}^{(0)}_{,1} + \mathbf{A}_{13}\mathbf{u}^{(0)}_{,3} + \mathbf{A}_{11}\mathbf{u}^{(1)}_{,y}]_{,1} + [\mathbf{A}_{31}\mathbf{u}^{(0)}_{,1} + \mathbf{A}_{33}\mathbf{u}^{(0)}_{,3} + \mathbf{A}_{31}\mathbf{u}^{(1)}_{,y}]_{,3} + [\mathbf{A}_{11}\mathbf{u}^{(2)}_{,y} + \mathbf{A}_{11}\mathbf{u}^{(1)}_{,1} + \mathbf{A}_{13}\mathbf{u}^{(1)}_{,3}]_{,y} = 0, & x_3 < h(y) \\ -h_y\mathbf{A}_{11}\mathbf{u}^{(2)}_{,y} - h_y\mathbf{A}_{11}\mathbf{u}^{(1)}_{,1} - h_y\mathbf{A}_{13}\mathbf{u}^{(1)}_{,3} + \mathbf{A}_{31}\mathbf{u}^{(1)}_{,y} + \mathbf{A}_{31}\mathbf{u}^{(0)}_{,1} + \mathbf{A}_{33}\mathbf{u}^{(0)}_{,3} = 0, & x_3 = h(y) \end{cases} \tag{B2}$$

Order ε^{1}:

$$\begin{cases} [\mathbf{A}_{11}\mathbf{u}^{(1)}_{,1} + \mathbf{A}_{13}\mathbf{u}^{(1)}_{,3} + \mathbf{A}_{11}\mathbf{u}^{(2)}_{,y}]_{,1} + [\mathbf{A}_{31}\mathbf{u}^{(1)}_{,1} + \mathbf{A}_{31}\mathbf{u}^{(2)}_{,y} + \mathbf{A}_{33}\mathbf{u}^{(1)}_{,3}]_{,3} + [\mathbf{A}_{11}\mathbf{u}^{(2)}_{,1} + \mathbf{A}_{13}\mathbf{u}^{(2)}_{,3}]_{,y} = 0, & x_3 < h(y) \\ -h_y\mathbf{A}_{11}\mathbf{u}^{(2)}_{,1} - h_y\mathbf{A}_{13}\mathbf{u}^{(2)}_{,3} + \mathbf{A}_{31}\mathbf{u}^{(2)}_{,y} + \mathbf{A}_{31}\mathbf{u}^{(1)}_{,1} + \mathbf{A}_{33}\mathbf{u}^{(1)}_{,3} = 0, & x_3 = h(y) \end{cases} \tag{B3}$$

order ε^{2}:

$$\begin{cases} \mathbf{A}_{11}\mathbf{u}^{(2)}_{,11} + \mathbf{A}_{13}\mathbf{u}^{(2)}_{,31} + \mathbf{A}_{31}\mathbf{u}^{(2)}_{,13} + \mathbf{A}_{33}\mathbf{u}^{(2)}_{,33} = 0, & x_3 < h(y) \\ \mathbf{A}_{31}\mathbf{u}^{(2)}_{,1} + \mathbf{A}_{33}\mathbf{u}^{(2)}_{,3} = 0, & x_3 = h(y) \end{cases} \tag{B4}$$

Based on Eq. (B1), we suggest the following form for $\mathbf{u}^{(1)}$:

$$\mathbf{u}^{(1)} = \mathbf{N}^{1}\mathbf{u}^{(0)} + \mathbf{N}^{11}\mathbf{u}^{(0)}_{,1} + \mathbf{N}^{13}\mathbf{u}^{(0)}_{,3} \tag{B5}$$

Where $\mathbf{N}^{1}$, $\mathbf{N}^{11}$, $\mathbf{N}^{13}$ are 2×2 matrices, functions of x_3 and y, periodic in y with period 1.

Implementing Eqs. (B5) into (B1) yields:

$$\begin{aligned} [\mathbf{A}_{11}\mathbf{u}^{(1)}_{,y} + \mathbf{A}_{11}\mathbf{u}^{(0)}_{,1} + \mathbf{A}_{13}\mathbf{u}^{(0)}_{,3}]_{,y} = [\mathbf{A}_{11}(\mathbf{N}^{1}_{,y}\mathbf{u}^{(0)} + \mathbf{N}^{11}_{,y}\mathbf{u}^{(0)}_{,1} + \mathbf{N}^{13}_{,y}\mathbf{u}^{(0)}_{,3} \\ + \mathbf{N}^{133}_{,y}\mathbf{u}^{(0)}_{,33} + \mathbf{N}^{0}_{,y}) + \mathbf{A}_{11}\mathbf{u}^{(0)}_{,1} \\ + \mathbf{A}_{13}\mathbf{u}^{(0)}_{,3}]_{,y}, \quad x_3 < h(y) \end{aligned} \tag{B6}$$

$$\begin{aligned} h_y[-\mathbf{A}_{11}(\mathbf{N}^{1}_{,y}\mathbf{u}^{(0)} + \mathbf{N}^{11}_{,y}\mathbf{u}^{(0)}_{,1} + \mathbf{N}^{13}_{,y}\mathbf{u}^{(0)}_{,3} + \mathbf{N}^{133}_{,y}\mathbf{u}^{(0)}_{,33} + \mathbf{N}^{0}_{,y}) \\ - \mathbf{A}_{11}\mathbf{u}^{(0)}_{,1} - \mathbf{A}_{13}\mathbf{u}^{(0)}_{,3}] = 0, \quad x_3 = h(y) \end{aligned} \tag{B7}$$

Gathering the coefficients of $\mathbf{u}^{(0)}$, $\mathbf{u}^{(0)}_{,1}$, $\mathbf{u}^{(0)}_{,3}$, and $\mathbf{u}^{(0)}_{,33}$ and from the remaining constants, we get the following systems for $\mathbf{N}^{1}$, $\mathbf{N}^{11}$, and $\mathbf{N}^{13}$:

$$\begin{cases} [\mathbf{A}_{11}\mathbf{N}^{1}_{,y}]_{,y} = 0, & x_3 < h(y) \\ -h_y\mathbf{A}_{11}\mathbf{N}^{1}_{,y} = 0, & x_3 = h(y) \end{cases} \tag{B8}$$

$$\begin{cases} [\mathbf{A}_{11}\mathbf{N}^{11}_{,y} + \mathbf{A}_{11}]_{,y} = 0, & x_3 < h(y) \\ \mathbf{A}_{11}\mathbf{N}^{11}_{,y} + \mathbf{A}_{11} = 0, & x_3 = h(y) \end{cases} \tag{B9}$$

$$\begin{cases} [\mathbf{A}_{11}\mathbf{N}^{13}_{,y} + \mathbf{A}_{13}]_{,y} = 0, & x_3 < h(y) \\ -h_y(\mathbf{A}_{11}\mathbf{N}^{13}_{,y} + \mathbf{A}_{13}) = , & x_3 = h(y) \end{cases} \tag{B10}$$

which can be solved to obtain the following expressions for the $\mathbf{N}^{i}_{,y}$, $i \in \{1, 11, 13\}$:

$$\mathbf{N}^{1}_{,y} = 0, \quad x_3 \le h(y) \tag{B11}$$

$$\mathbf{N}^{11}_{,y} = \begin{cases} 0, & x_3 < h(y) \\ -\mathbf{I}, & x_3 = h(y) \end{cases} \tag{B12}$$

$$\mathbf{N}^{13}_{,y} = \begin{cases} \mathbf{A}_{11}^{-1}\langle \mathbf{A}_{11}^{-1}\rangle^{-1}\langle \mathbf{A}_{11}^{-1}\mathbf{A}_{13}\rangle - \mathbf{A}_{11}^{-1}\mathbf{A}_{13}, & x_3 < h(y) \\ -\mathbf{A}_{11}^{-1}\mathbf{A}_{13}, & x_3 = h(y) \end{cases} \tag{B13}$$

where $\langle\cdot\rangle = \int_0^1 \cdot\, dy = \int_0^{y_1} \cdot\, dy + \int_{y_2}^1 \cdot\, dy$.

We integrate the bulk equation in system (B2) over y from 0 to 1, and by a process similar to the one presented in Sec. 4, we get the following equilibrium equation in the effective layer

$$\begin{aligned} &\langle \mathbf{A}_{11}\rangle\mathbf{u}^{(0)}_{,11} + \mathbf{A}_{13}\mathbf{u}^{(0)}_{,31} + [\langle \mathbf{A}_{31}\rangle\mathbf{u}^{(0)}_{,1}]_{,3} + [\langle \mathbf{A}_{33}\rangle\mathbf{u}^{(0)}_{,3}]_{,3} \\ &\quad = (y_2' - y_1')(\mathbf{A}_{33} - \mathbf{A}_{31}\mathbf{A}_{11}^{-1}\mathbf{A}_{13})]\mathbf{u}^{(0)}_{,3}, \quad -\frac{\delta}{2} < x_3 < \frac{\delta}{2} \end{aligned} \tag{B14}$$

Comparing it to

$$\begin{aligned} &\mathbf{A}^{eff}_{11}\mathbf{u}^{(0)}_{,11} + \mathbf{A}^{eff}_{13}\mathbf{u}^{(0)}_{,31} + [\mathbf{A}^{eff}_{31}\mathbf{u}^{(0)}_{,1}]_{,3} + [\mathbf{A}^{eff}_{33}\mathbf{u}^{(0)}_{,3}]_{,3} = \mathbf{D}^{eff}_{3}\mathbf{u}^{(0)}_{,3}, \\ &\quad -\frac{\delta}{2} < x_3 < \frac{\delta}{2} \end{aligned} \tag{B15}$$

we get the effective properties as

$$\mathbf{A}^{eff}_{11} = \begin{bmatrix} (\lambda+2\mu)(1-y_2+y_1) & 0 \\ 0 & \mu(1-y_2+y_1) \end{bmatrix}, \quad \mathbf{A}^{eff}_{13} = \begin{bmatrix} 0 & \lambda \\ \mu & 0 \end{bmatrix} \tag{B16}$$

$$\begin{aligned} \mathbf{A}^{eff}_{31} &= \begin{bmatrix} 0 & \mu(1-y_2+y_1) \\ \lambda(1-y_2+y_1) & 0 \end{bmatrix}, \\ \mathbf{A}^{eff}_{33} &= \begin{bmatrix} (1-y_2+y_1)\mu & 0 \\ 0 & (1-y_2+y_1)(\lambda+2\mu) \end{bmatrix} \end{aligned} \tag{B17}$$

$$\mathbf{D}^{eff}_{3} = \begin{bmatrix} 0 & 0 \\ 0 & \dfrac{4\mu(\lambda+\mu)}{\lambda+2\mu}(y_2' - y_1') \end{bmatrix} \tag{B18}$$

Then, we calculate the effective Young's modulus of a thin film similar to the one presented in Sec. 5.

$$\sigma_{13} = C_{1311}\varepsilon_{11} + C_{1313}\varepsilon_{13} + C_{1331}\varepsilon_{31} + C_{1333}\varepsilon_{33} = 2\mu f(x_3)\varepsilon_{13} = 0 \tag{B19}$$

$$\begin{aligned} \sigma_{33} &= C_{3311}\varepsilon_{11} + C_{3313}\varepsilon_{13} + C_{3331}\varepsilon_{31} + C_{3333}\varepsilon_{33} \\ &= \lambda f(x_3)\varepsilon_{11} + f(x_3)(\lambda+2\mu)\varepsilon_{33} = 0 \end{aligned} \tag{B20}$$

(B19) and (B20) give the following relations between the strain tensor components:

$$\varepsilon_{33} = \frac{-\lambda}{(\lambda + 2\mu)} \varepsilon_{11} \tag{B21}$$

$$\varepsilon_{13} = 0 \tag{B22}$$

From Eqs. (B21) and (B22), we get the remaining stress tensor components in terms of ε_{11}:

$$\begin{aligned} \sigma_{11} &= C_{1111}\varepsilon_{11} + C_{1113}\varepsilon_{13} + C_{1131}\varepsilon_{31} + C_{1133}\varepsilon_{33} \\ &= \left[(\lambda + 2\mu)f(x_3) - \frac{\lambda^2}{\lambda + 2\mu}\right]\varepsilon_{11} \end{aligned} \tag{B23}$$

$$\sigma_{31} = C_{3111}\varepsilon_{11} + C_{3113}\varepsilon_{13} + C_{3131}\varepsilon_{31} + C_{3133}\varepsilon_{33} = 0 \tag{B24}$$

Therefore, by Eqs. (B21)–(B24), the strain energy density in the layer is

$$W_{layer} = \frac{1}{2} A \varepsilon_{11}^2 \int_{-(\delta/2)}^{\delta/2} \left[(\lambda + 2\mu)f(x_3) - \frac{\lambda^2}{\lambda + 2\mu}\right] dx_3 \tag{B25}$$

Adding the strain energy density in the bulk and then using Eq. (69), we get the renormalized Young's modulus for the thin film due to surface roughness in the absence of surface elasticity:

$$E^{eff} = \frac{4\mu(\lambda + \mu)}{\lambda + 2\mu} - \frac{\lambda + 2\mu}{2} \frac{\delta}{h} \tag{B26}$$

References

[1] Haiss, W., 2001, "Surface Stress of Clean and Adsorbate-Covered Solids," Rep. Prog. Phys., **64**(5), pp. 591–648.
[2] Müller, P., and Saúl, A., 2004, "Elastic Effects on Surface Physics," Surf. Sci. Rep., **54**(5–8), pp. 157–258.
[3] Pala, R. G. S., and Liu, F., 2004, "Determining the Adsorptive and Catalytic Properties of Strained Metal Surfaces Using Adsorption-induced Stress," J. Chem. Phys., **120**(16), pp. 7720–7724.
[4] Wang, G.-F., and Feng, X.-Q., 2007, "Effects of Surface Elasticity and Residual Surface Tension on the Natural Frequency of Micro Beams," Appl. Phys. Lett., **90**(23), p. 231904.
[5] Park, H. S., 2008, "Strain Sensing Through the Resonant Properties of Deformed Metal Nanowires," J. Appl. Phys., **104**(1), p. 013516.
[6] Park, H. S., 2009, "Quantifying the Size-dependent Effect of the Residual Surface Stress on the Resonant Frequencies of Silicon Nanowires If Finite Deformation Kinematics Are Considered," J. Mech. Phys. Solids, **56**(11), pp. 3144–3166.
[7] Sharma, P., Ganti, S., and Bhate, N., 2003, "Effect of Surfaces on the Size-Dependent Elastic State of Nano-Inhomogeneities," Appl. Phys. Lett., **82**(4), pp. 535–537.
[8] Duan, H., Wang, J., Huang, Z., and Karihaloo, B. L., 2005, "Size-Dependent Effective Elastic Constants of Solids Containing Nano-Inhomogeneities With Interface Stress," J. Mech. Phys. Solids, **53**(7), pp. 1574–1596.
[9] Huang, Z. P., and Sun, L., 2007, "Size-Dependent Effective Properties of a Heterogeneous Material With Interface Energy Effect: From Finite Deformation Theory to Infinitesimal Strain Analysis," Acta Mech., **190**(1–4), pp. 151–163.
[10] Mogilevskaya, S. G., Crouch, S. L., and Stolarski, H. K., 2008, "Multiple Interacting Circular Nano-Inhomogeneities With Surface/interface Effects," J. Mech. Phys. Solids, **56**(6), pp. 2298–2327.
[11] Suo, Z., and Lu, W., 2000, "Forces That Drive Nanoscale Self-Assembly on Solid Surfaces," J. Nanopart. Res., **2**(4), pp. 333–344.
[12] Diao, J., Gall, K., and Dunn, M. L., 2003, "Surface-Stress-Induced Phase Transformation in Metal Nanowires," Nat. Mater., **2**(10), pp. 656–660.
[13] Fischer, F., Waitz, T., Vollath, D., and Simha, N., 2008, "On the Role of Surface Energy and Surface Stress in Phase-Transforming Nanoparticles," Prog. Mater. Sci., **53**(3), pp. 481–527.
[14] Gorbushin, N., Eremeyev, V. A., and Mishuris, G., 2020, "On Stress Singularity Near the Tip of a Crack With Surface Stresses," Int. J. Eng. Sci., **146**, p. 103183.
[15] Miller, R. E., and Shenoy, V. B., 2000, "Size-Dependent Elastic Properties of Nanosized Structural Elements," Nanotechnology, **11**(3), pp. 139–147.
[16] Diao, J., Gall, K., Dunn, M. L., and Zimmerman, J. A., 2006, "Atomistic Simulations of the Yielding of Gold Nanowires," Acta Mater., **54**(3), pp. 643–653.
[17] Villain, P., Beauchamp, P., Badawi, K., Goudeau, P., and Renault, P.-O., 2004, "Atomistic Calculation of Size Effects on Elastic Coefficients in Nanometre-Sized Tungsten Layers and Wires," Scr. Mater., **50**(9), pp. 1247–1251.
[18] Dingreville, R., Qu, J., and Cherkaoui, M., 2005, "Surface Free Energy and Its Effect on the Elastic Behavior of Nano-sized Particles, Wires and Films," J. Mech. Phys. Solids, **53**(8), pp. 1827–1854.
[19] Jing, G. Y., Duan, H. L., Sun, X. M., Zhang, Z. S., Xu, J., Li, Y. D., Wang, J. X., and Yu, D. P., 2006, "Surface Effects on Elastic Properties of Silver Nanowires: Contact Atomic-Force Microscopy," Phys. Rev. B, **73**(23), p. 235409.
[20] Lachut, M. J., and Sader, J. E., 2007, "Effect of Surface Stress on the Stiffness of Cantilever Plates," Phys. Rev. Lett., **99**(20), p. 206102.
[21] Liu, C., and Rajapakse, R. K. N. D., 2010, "Continuum Models Incorporating Surface Energy for Static and Dynamic Response of Nanoscale Beams," IEEE Trans. Nanotechnol., **9**(4), pp. 422–431.
[22] Bar On, B., Altus, E., and Tadmor, E., 2010, "Surface Effects in Non-uniform Nanobeams: Continuum Vs. Atomistic Modeling," Int. J. Solids Struct., **47**(9), pp. 1243–1252.
[23] Wang, Z.-Q., Zhao, Y.-P., and Huang, Z.-P., 2010, "The Effects of Surface Tension on the Elastic Properties of Nano Structures," Int. J. Eng. Sci., **48**(2), pp. 140–150.
[24] De Gennes, P.-G., Brochard-Wyart, F., and Quéré, D., 2013, *Capillarity and Wetting Phenomena: Drops, Bubbles, Pearls, Waves*, Springer Science & Business Media, New York.
[25] Style, R. W., Hyland, C., Boltyanskiy, R., Wettlaufer, J. S., and Dufresne, E. R., 2013, "Surface Tension and Contact With Soft Elastic Solids," Nat. Commun., **4**(1), pp. 1–6.
[26] Style, R. W., Jagota, A., Hui, C.-Y., and Dufresne, E. R., 2017, "Elastocapillarity: Surface Tension and the Mechanics of Soft Solids," Annu. Rev. Condens. Matter Phys., **8**(1), pp. 99–118.
[27] Krichen, S., Liu, L., and Sharma, P., 2019, "Liquid Inclusions in Soft Materials: Capillary Effect, Mechanical Stiffening and Enhanced Electromechanical Response," J. Mech. Phys. Solids, **127**(1), pp. 332–357.
[28] Biria, A., Maleki, M., and Fried, E., 2013, "Continuum Theory for the Edge of an Open Lipid Bilayer," *Advances in Applied Mechanics*, Vol. 46, S.P.A. Bordas, ed., Elsevier, San Diego, CA, pp. 1–68.
[29] Liu, L., Yu, M., Lin, H., and Foty, R., 2017, "Deformation and Relaxation of An Incompressible Viscoelastic Body With Surface Viscoelasticity," J. Mech. Phys. Solids, **98**(3), pp. 309–329.
[30] Gurtin, M. E., and Murdoch, A. I., 1975, "A Continuum Theory of Elastic Material Surfaces," Arch. Ration. Mech. Anal., **57**(4), pp. 291–323.
[31] Gurtin, M., Weissmüller, J., and Larche, F., 1998, "A General Theory of Curved Deformable Interfaces in Solids At Equilibrium," Philos. Mag. A, **78**(5), pp. 1093–1109.
[32] Mozaffari, K., Yang, S., and Sharma, P., 2019, *Surface Energy and Nanoscale Mechanics* (Handbook of Materials Modeling), Springer Nature, Switzerland, pp. 1–26.
[33] Li, S., and Wang, G., 2008, *Introduction to Micromechanics and Nanomechanics*, World Scientific Publishing Company, Hackensack, NJ.
[34] Cammarata, R. C., 2009, "Generalized Thermodynamics of Surfaces With Applications to Small Solid Systems," Solid State Phys., **61**, pp. 1–75.
[35] Duan, H., Wang, J., and Karihaloo, B. L., 2009, "Theory of Elasticity at the Nanoscale," *Advances in Applied Mechanics*, Vol. 42, H. Aref, and E. van der Giessen, eds., Elsevier, San Diego, CA, pp. 1–68.
[36] Javili, A., McBride, A., and Steinmann, P., 2013, "Thermomechanics of Solids With Lower-dimensional Energetics: On the Importance of Surface, Interface, and Curve Structures at the Nanoscale. A Unifying Review," Appl. Mech. Rev., **65**(1), p. 010802.
[37] Hashin, Z., 2002, "Thin Interphase/imperfect Interface in Elasticity With Application to Coated Fiber Composites," J. Mech. Phys. Solids, **50**(12), pp. 2509–2537.
[38] Brisard, S., Dormieux, L., and Kondo, D., 2010, "Atomistic Calculations of Elastic Properties of Metallic FCC Crystal Surfaces," Comput. Mater. Sci., **48**(3), pp. 589–596.
[39] Steigmann, D. J., and Ogden, R. W., 1997, "Plane Deformations of Elastic Solids With Intrinsic Boundary Elasticity," Proc. R. Soc. Lond. Ser. A: Math. Phys. Eng. Sci., **453**(1959), pp. 853–877.
[40] Steigmann, D. J., and Ogden, R. W., 1999, "Elastic Surface-Substrate Interactions," Proc. R. Soc. Lond. Ser. A: Math. Phys. Eng. Sci., **455**(1982), pp. 437–474.
[41] Fried, E., and Todres, R. E., 2005, "Mind the Gap: The Shape of the Free Surface of a Rubber-Like Material in Proximity to a Rigid Contactor," J. Elast., **80**(1–3), pp. 97–151.
[42] Schiavone, P., and Ru, C. Q., 2009, "Solvability of Boundary Value Problems in a Theory of Plane-Strain Elasticity With Boundary Reinforcement," Int. J. Eng. Sci., **47**(11–12), pp. 1331–1338.
[43] Chhapadia, P., Mohammadi, P., and Sharma, P., 2011, "Curvature-dependent Surface Energy and Implications for Nanostructures," J. Mech. Phys. Solids, **59**(10), pp. 2103–2115.
[44] Weissmuller, J., and Duan, H., 2008, "Cantilever Bending With Rough Surfaces," Phys. Rev. Lett., **101**(14), p. 146102.
[45] Wang, Y., Weissmuller, J., and Duan, H., 2010, "Mechanics of Corrugated Surfaces," J. Mech. Phys. Solids, **58**(10, pp. 1552–1566.
[46] Mohammadi, P., Liu, L. P., Sharma, P., and Kukta, R. V., 2013, "Surface Energy, Elasticity and the Homogenization of Rough Surfaces," J. Mech. Phys. Solids, **61**(2), pp. 325–340.
[47] Nevard, J., and Keller, J. B., 1997, "Homogenization of Rough Boundaries and Interfaces," SIAM J. Appl. Math., **57**(6), pp. 1660–1686.
[48] Vinh, P. C., and Tung, D. X., 2010, "Homogenized Equations of the Linear Elasticity in Two-Dimensional Domains with Very Rough Interfaces," Mech. Res. Commun., **37**(3), pp. 285–288.

[49] Vinh, P. C., Tung, D. X., and Kieu, N. T., 2018, "Homogenization of Very Rough Two-Dimensional Interfaces Separating Two Dissimilar Poroelastic Solids With Time-Harmonic Motions," Math. Mech. Solids, **24**(5), pp. 1349–1367.
[50] Le Quang, H., He, Q. C., and Le, H. T., 2013, "Multiscale Homogenization of Elastic Layered Composites With Unidirectionally Periodic Rough Interfaces," Multiscale Model. Simul., **11**(4), pp. 1127–1148.
[51] Le, H. T., Le Quang, H., and He, Q.-C., 2014, "The Effective Elastic Moduli of Columnar Composites Made of Cylindrically Anisotropic Phases With Rough Interfaces," Int. J. Solids Struct., **51**(14), pp. 2633–2647.
[52] Elsner, B., Muller, S., Bargmann, S., and Weissmuller, J., 2017, "Surface Excess Elasticity of Gold: Ab Initio Coefficients and Impact on the Effective Elastic Response of Nanowires," Acta Mater., **124**(6), pp. 468–477.
[53] Kohler, W., Papanicolaou, G., and Varadhan, S., 1981, "Boundary and Interface Problems in Regions with Very Rough Boundaries," *Multiple Scattering and Waves in Random Media*, P. L. Chow, W. E. Kohler, and G. C. Papanicolaou, eds., North-Holland Publishing Company, Amsterdam, p. 165.
[54] Love, A., 1944, *A Treatise on the Mathematical Theory of Elasticity* (Dover Books on Engineering Series), Dover Publications.
[55] Shenoy, V. B., 2005, "Atomistic Calculations of Elastic Properties of Metallic FCC Crystal Surfaces," Phys. Rev. B, **71**(9), p. 094104.